Abstract

The Yamato Sanmyaku is a mountain range located at about 200 km south of the Prins Harald Kyst, East Antarctica. The range forms an arcuate chain, extending 50 km north-south, comprising seven massifs temporarily named A, B, C, D, E, F and G. The rocks of the area are divided into a charnockitic group (pyroxene gneisses and pyroxene syenites) and a granitic group (migmatitic gneisses, granitic gneiss, and microcline granites). In addition, metabasite inter-layers and metadikes are found everywhere, associated with microcline pegmatites. The charnockitic group is involved in the older complex which crystallized under the conditions of a granulite facies. It has been partly modified by later granitization related to the granitic group which itself shows various stages of granitization. The grade of metamorphism increases towards the north, parallel to the gneissosity. The intercalated metabasite layers correspond to the host rocks in mineral paragenesis.

Basic dikes are intruded obliquely into both the granitic gneisses and the pyroxene syenites, and are metamorphosed into various metabasites under the conditions of an amphibolite facies. This metamorphism is probably related to the subsequent intrusion of microcline granites and associated microcline pegma-tite. A thrust movement from east to west represents the last stage of the structural evolution.

I. INTRODUCTION

The Yamato Sanmyaku is a mountain range located between 32°25' E, 71° 14' S and 36°05' E, 71°45' S, about 200 km south of the Prins Harald Kyst, East Antarctica.

These mountains, exploration of which was the goal of the fourth Japanese Antarctic Research Expedition (JARE IV-1960), were discovered from the air in 1937 by a Norwegian party headed by Lars CHRISTENSEN during the exploration of the coast. Oblique photographs were taken from the air by a Belgian party on the way to Syowa Station in the spring of 1960. Guided by information from these two sources, in the summer of 1960 a traverse party of the JARE IV reached the area and spent three weeks there. They made precise surveys of the area and preliminary studies of the geology, geomorphology and glaciology of the mountains. In 1961, during a traverse trip farther south, a party of the JARE V visited the same area and compiled detailed topographic maps (Fig. 1).
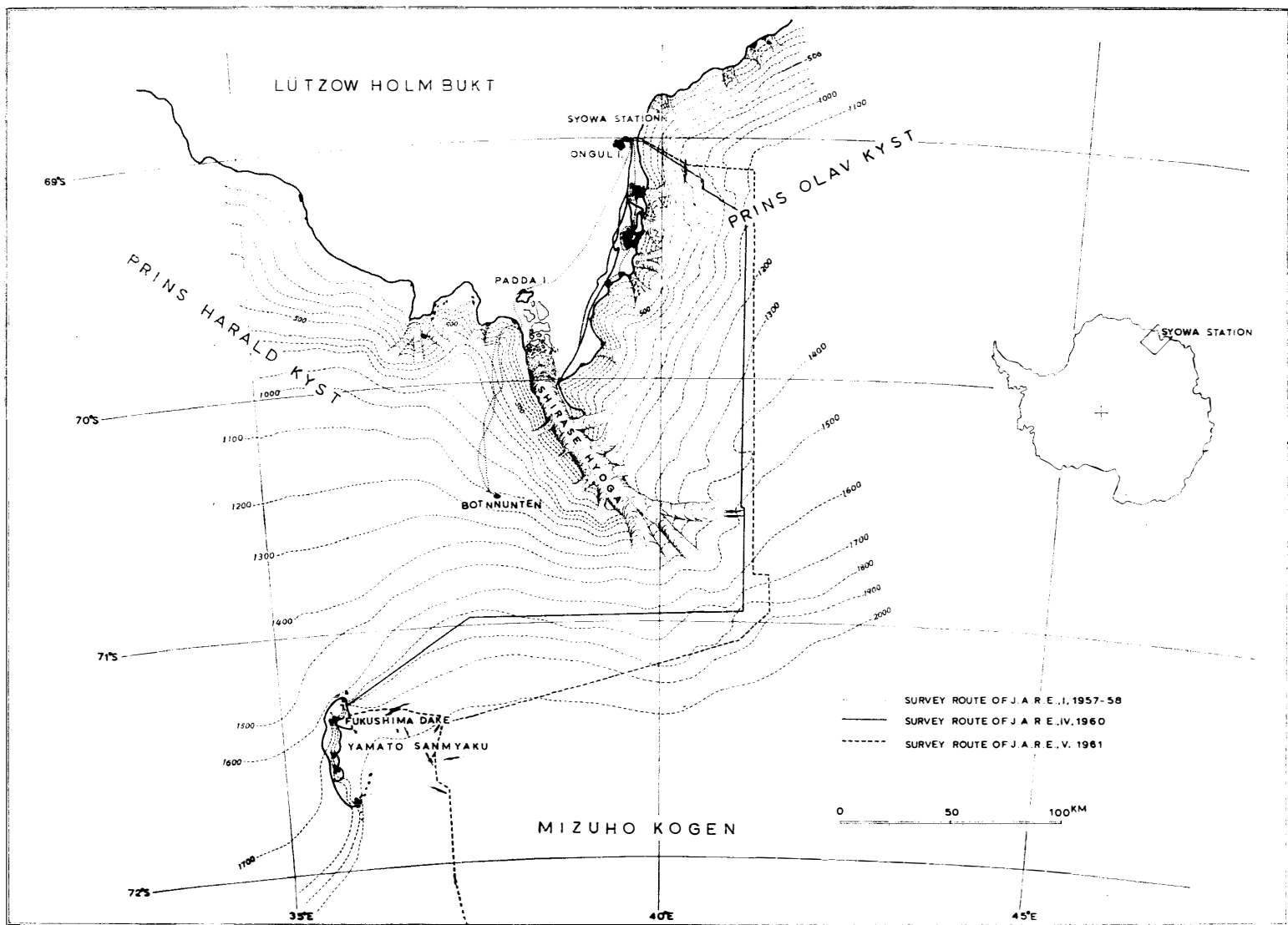
The field work on which this report is based was carried out by the writer as a member of the wintering party of the JARE IV-1960. As a detailed survey was impossible because of the limited time, the work was preliminary, and more detailed investigations are expected in future.

The Yamato Sanmyaku forms an arcuate mountain chain, composed of seven massifs, extending 50 km from north to south. These massifs are surrounded by nunataks and are separated from each other by several glaciers flowing from east to west. Because of the subglacial topography, a subordinate inner arc of small nunataks may be distinguished by the ice cliffs connecting these nunataks. This inner arc, which joins the main arc at massif A, extends 40-50 km farther south before it is covered by the ice sheet.

Because the ice sheets on opposite sides of the mountains are on different levels, the ice in the area flows from east to west. The difference in levels is about 300 m, and the surface of the ice sheet on the eastern side of the mountains is 1900-2000 m above sea level. On the western side, the ice flows to the north, as is indicated by the arrangement of the moraine deposits.

Massifs D, E, F and G in the northern area of the mountains show a steep "aiguille" topography. Massif D contains the highest peak 2360 m above sea level. This mountain has been named Fukushima Dake in memory of the late S. FUKUSHIMA, a geophysicist with the JARE IV party. In contrast to these

Fig. 1. JOURNEYS FOR GEOLOGICAL SURVEY OF J.A.R.E., 1957-1961

LÜTZOW HOLM BUKT

PRINS OLAV KYST

PRINS HARALD KYST

SYOWA STATION

ONGUL

PADDA I.

SHIRASE HYOGA

BOTNNUNTEN

SYOWA STATION

FUKUSHIMA DAKE
YAMATO SANMYAKU

MIZUHO KOGEN

69°S
70°S
71°S
72°S

35°E
40°E
45°E

.... SURVEY ROUTE OF J.A.R.E., I, 1957-58
———— SURVEY ROUTE OF J.A.R.E., IV, 1960
- - - - SURVEY ROUTE OF J.A.R.E., V, 1961

0   50   100 KM

steep northern massifs, massifs A, B, and C in the southern part of the mountains have comparatively gentle slopes and are partly covered by snow and moraines.

The geomorphology of the Yamato Sanmyaku has been described by YOSHIDA and FUJIWARA (1963). The present paper describes the petrography of the rocks from the Yamato Sanmyaku region. A charnockitic group and a granitic group, distinctly different in structural, petrochemical, and paragenetical features, are recognized. In order to determine the genesis and metamorphic grade of the rocks, optical measurements were made and the data thus obtained have also been used in describing some of the mineralogical features.
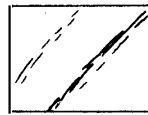
Fig. 2. GEOLOGICAL SKETCH MAP

G

60

F

30

P 40

E

40

30

2360

FUKUSHIMA DAKE

50

D
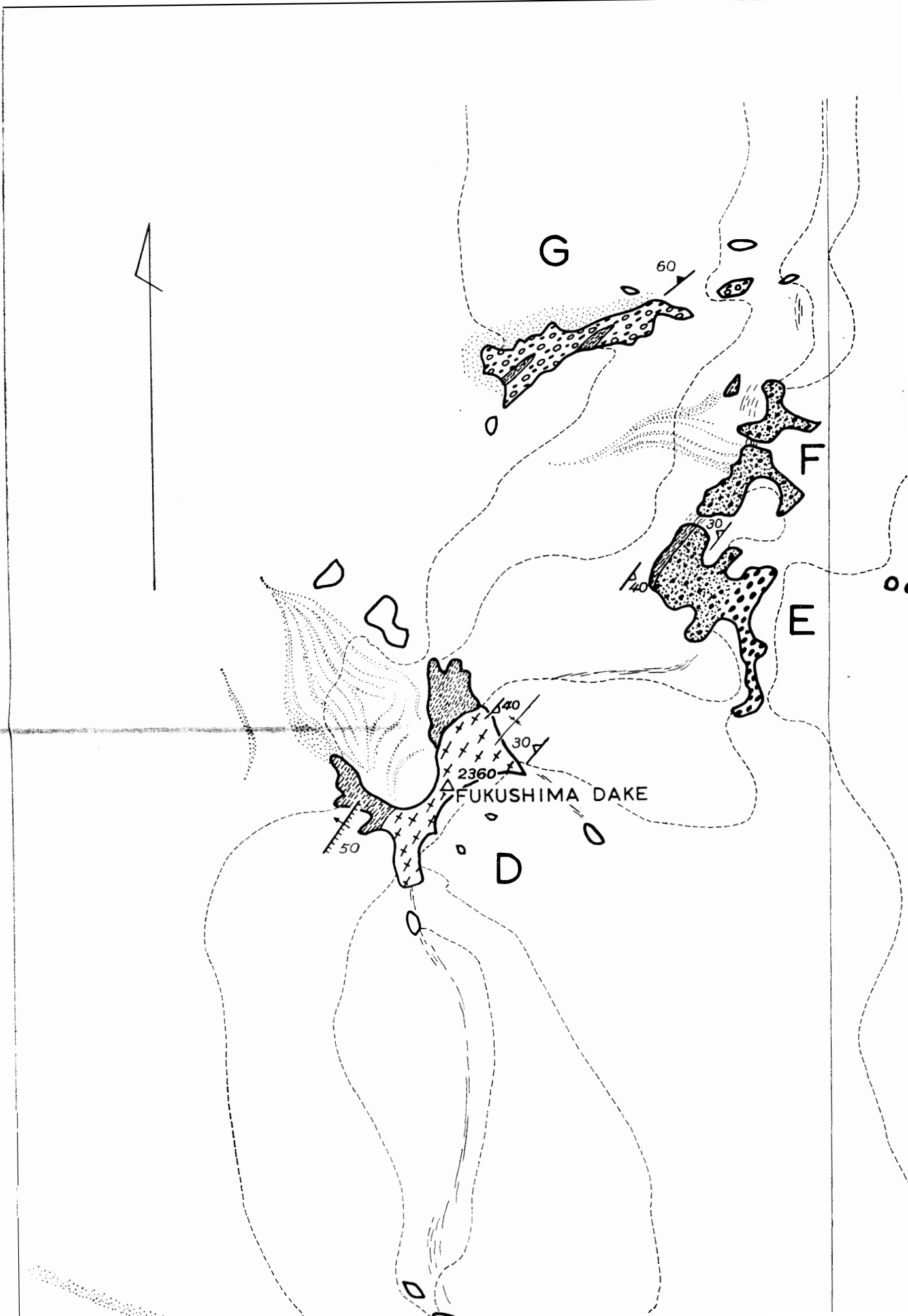
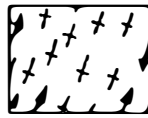# MAP OF YAMATO SANMYAKU
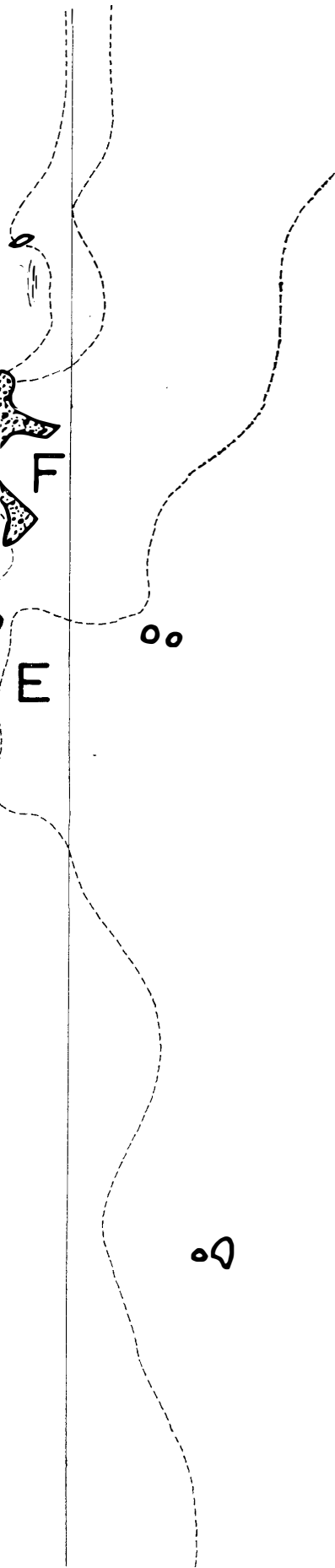
LEGEND

GLACIER

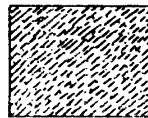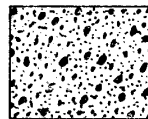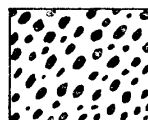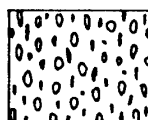MORAINE

GRANITIC GNEISS
(MICROCLINE GRANITE)

MIGMATIC GNEISS
(BIOTITE GRANITE)

PORPHYRITIC PYROXENE
SYENITE

PYROXENE SYENITE

PYROXENE GNEISS

METABASITE
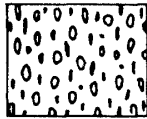
D

C

80

2100

1500

1600

30

30

B

D

oꝺ
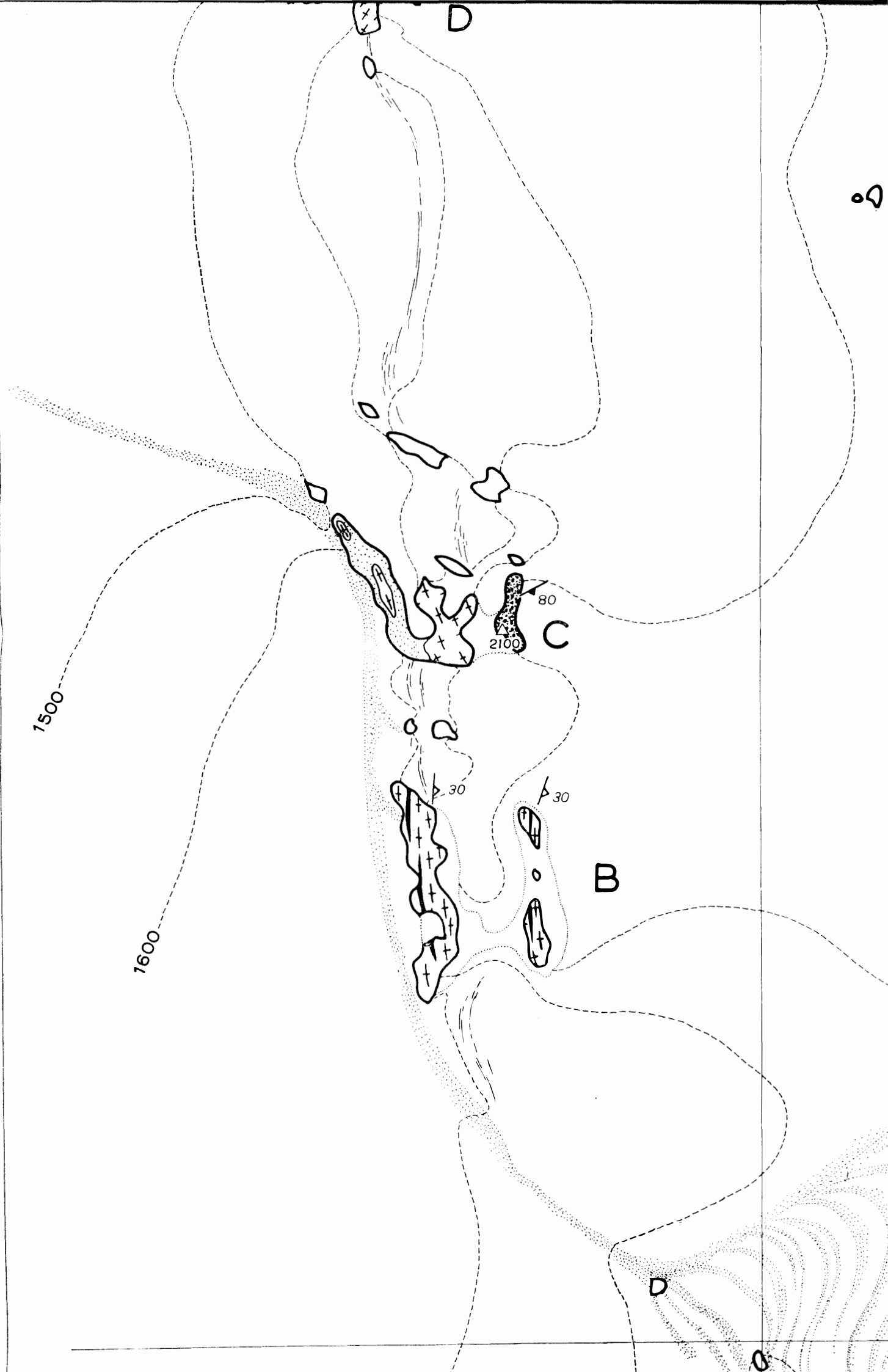
PYROXENE SYENITE

PYROXENE GNEISS

METABASITE

0 ————————————————————— 10KM

———————— 71°40'S

B

30

30

D

D

70
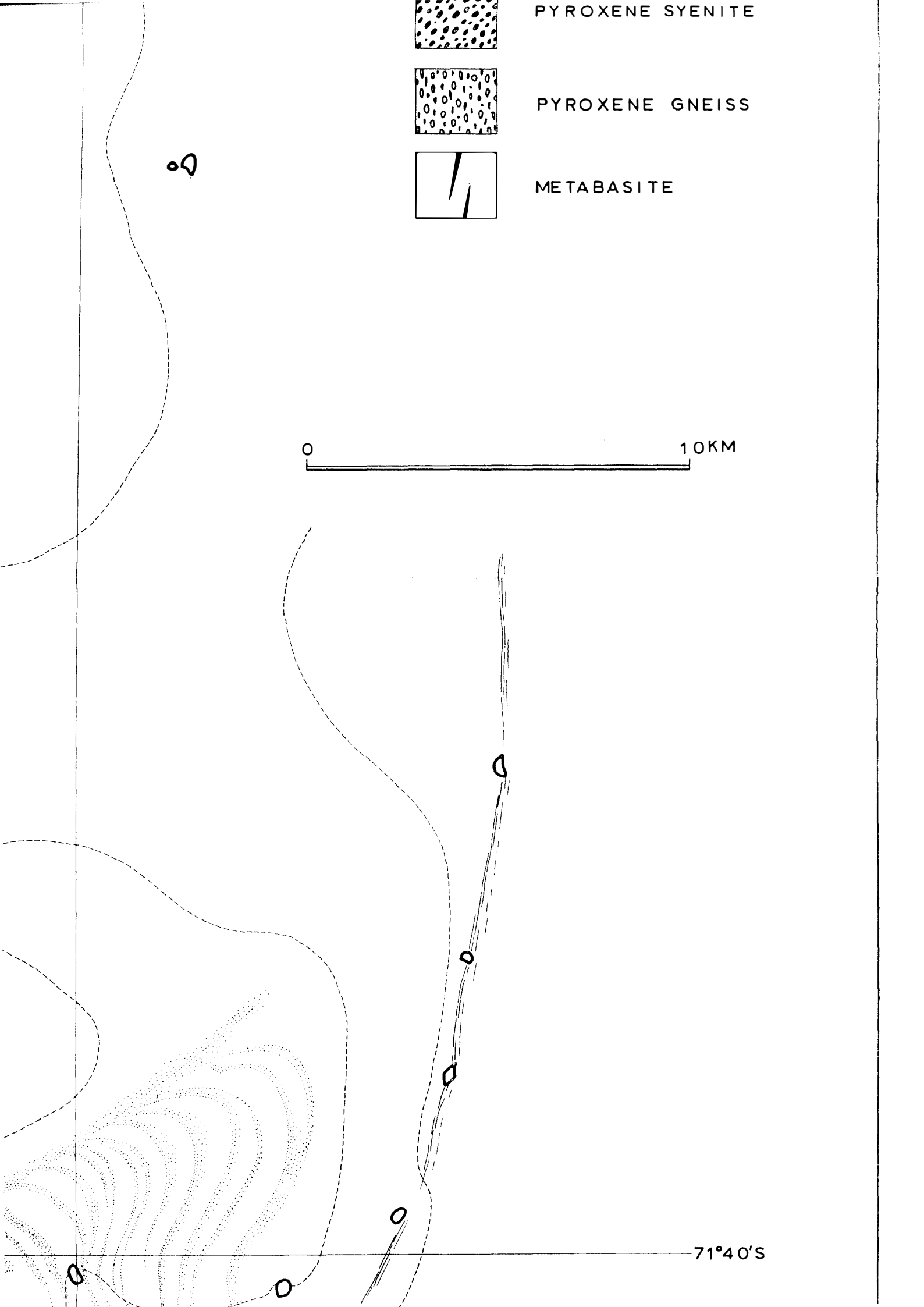
1500

1600

1700

1800

1900

35°45'E

71°4 0'S

1900

2000

35°45'E

70
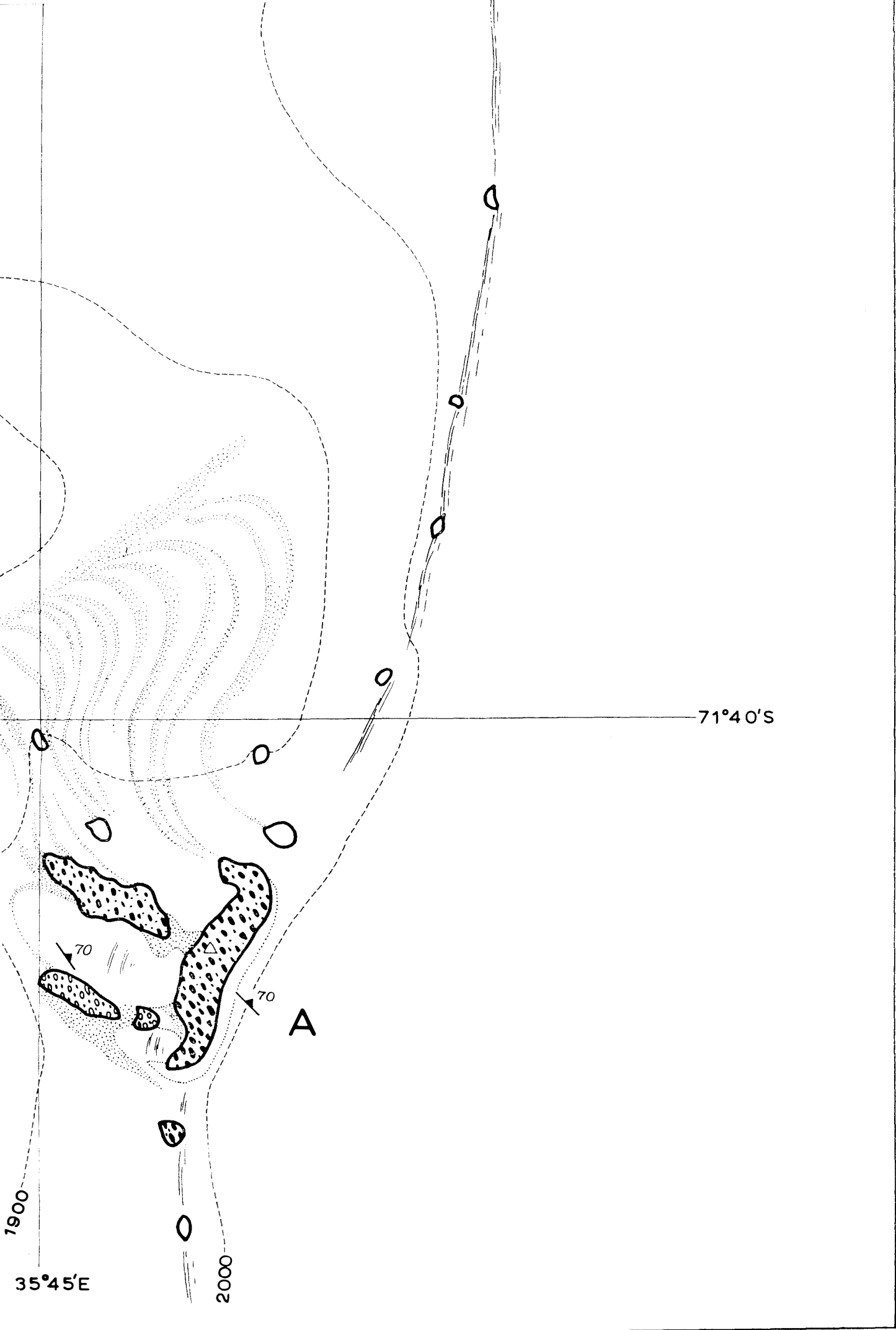
70

A

II. GEOLOGY

The Yamato Sanmyaku is involved in the basement complex of East Antarctica, and is composed of various gneisses and other plutonic rocks probably of lower Paleozoic age. Petrographically the mountains may be characterized by the rich development of migmatitic and syenitic rocks, in contrast to those on the Lützow-Holm Bukt coast where gneisses predominate.

The exposed rocks in the region may be classified as follows:
a) Pyroxene gneisses
b) Pyroxene syenites*
c) Migmatitic gneisses and biotite granites
d) Granitic gneisses
e) Microcline granites
f) Metabasites
g) Microcline pegmatites
h) Moraine deposits

The rocks are arranged more or less zonally, paralleling the mountain arc (Fig. 2).

Pyroxene gneisses and pyroxene syenites occur at the northern and southern ends of the mountain arc, and small masses of pyroxene syenite occur locally in the central part of the inner zone of the arc. Along the northern part of the outer zone, there are sheet-like, concordant intrusions of biotite granite in the pyroxene gneisses. In the southern part, angular fragments of this gneiss are included in the pyroxene syenite. In the northern part of the mountains, the relation between the pyroxene gneiss and the pyroxene syenite is not clear. The pyroxene gneisses and pyroxene syenites are referred to the charnockitic group from their mineralogy. The porphyritic pyroxene syenite grades into pink microcline granite with pyroxene relicts, showing no distinct boundary. In the central mountain area there are migmatitic gneisses, biotite granites and granitic gneisses. The migmatitic gneiss has a nebulitic, agmatitic appearance with many basic paleosomes. It has been granitized *in situ* into massive biotite granite. These granitic rocks are all characterized by purple-grey quartz grains.

The granitic gneisses occur as banded, augen, and nebulitic gneisses, repre-

---

* These rocks have been previously described as pyroxene granites
  (see. TATSUMI et al, 1963).

senting a granitization series similar to metablastesis and metatexis. The relation between the granitic gneiss and the pyroxene syenite is not clear, but the results of petrographical and structural investigations suggest that the granitic gneiss was produced by subsequent metamorphism and granitization of the pyroxene syenite.

The concordant sheets of microcline granites related to the granitization in the granitic gneiss area occur as discordant, small stocks in the pyroxene syenite area. These stocks are associated with pegmatite apophyses, controlled by the joint pattern, and represent a post-kinematic granite placed in the supracrustal rock, in this case, pyroxene syenite (Fig. 3).
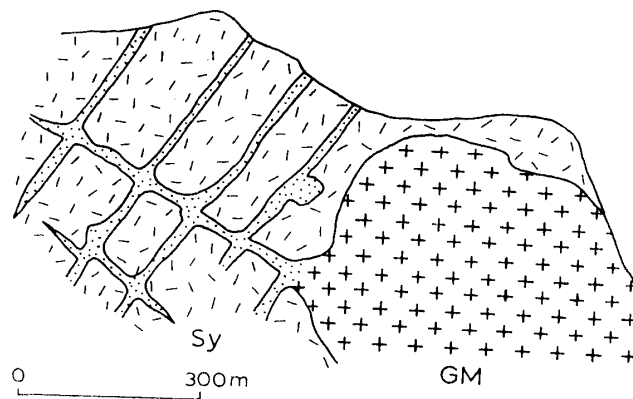
Fig. 3. Microcline granite stock (GM) and its pegmatite apophyses in the porphyritic pyroxene syenite (Sy) of massif C.

The metabasites which occur throughout this mountain area are of two types; metabasite bands or lenses that are more or less concordant with the country rocks, and metamorphosed basic dikes.

Microcline pegmatites are also widely distributed and are sometimes related to the microcline granite. In some places, these pegmatites were intruded subsequent to the emplacement of metabasite dikes.

In general the trend of the foliation of these rocks parallels the mountain arc. The dips are variable and some gentle folds are found in the granitic gneiss area. In Fig. 4, the poles of the foliations are plotted on a Schmidt's equal-area net. The dips of the charnockitic group clearly differ from those of the granitic group. The pyroxene gneisses and pyroxene syenites are steeply inclined, whereas the inclination of the granitic gneisses and migmatitic gneisses is more gentle. The poles of the foliations of the charnockitic group are more scattered than those of the granitic group. It is, therefore, conceivable that these two groups may have been involved in earlier and later tectonic events. This problem is discussed in the sections on petrography and petrochemistry.

Thrust faults are associated with a shear zone which strikes N 20° E and dips 50° E. The amount of dislocation on the thrusts is rather small. The gneiss, however, is sheared and granulated in places parallel to the fault zone, and the basic inclusions show an S-shaped rotation resulting from differential movements
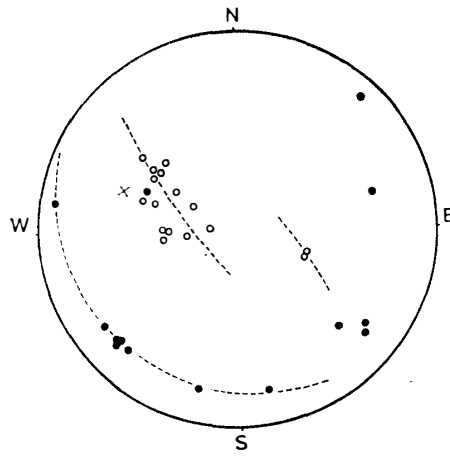
Fig. 4. Poles of measured foliation in the Yamato Sanmyaku region plotted on Schmidt's net.

　　　○　Granitic group.
　　　●　Charnockitic group.
　　　×　Pole of thrust plane.

along the thrust.

The radiogenic age of the granitic gneiss, which granitized from the pyroxene syenite, has been determined as 4.57×10^8 years (Sr-Rb method) by E. PICCIOTTO ct A. COPPEZ (1964). This value suggests that the age of the granitization may be lower Paleozoic.

8

III. PETROGRAPHY

a) Pyroxene gneisses

There are three species of pyroxene gneisses; pyroxene-biotite, enderbitic, and charnockitic. The pyroxene-biotite gneisses are usually found as basic inclusions (paleosomes) in pyroxene gneisses and pyroxene syenites. These inclusions are dark brown pyroxene-biotite gneisses, and fine-grained, dark green pyroxene amphibolites. In the enderbitic gneiss, the pyroxene-biotite gneisses occur as lenticular bands and boudins paralleling the gneissosity of the country rock. In the pyroxene syenite they are scattered in angular fragments. In the pyroxene syenite they are scattered in angular fragments. These gneisses have a fine-grained, granular texture and the constituents show preferred orientations; they have a banded, sometimes schistose, structure, characterized by potassium-feldspar and reddish-brown biotite associated with a small amount of pyroxene (Table 1).

Enderbitic gneisses occur in the western part of massif A. These gneisses are foliated and heterogeneous, and have many agmatitic inclusions of pyroxene-biotite gneisses and pyroxene amphibolites. The rocks are rather dark, brownish-grey and medium-grained, resembling enderbite defined by TILLEY (1930). They are composed primarily of plagioclase, with some pyroxene and biotite. Their
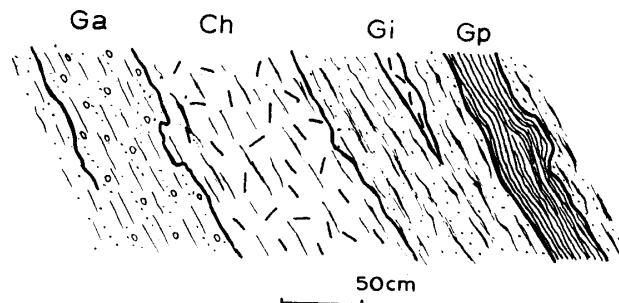
Fig, 5. Banded structure of charnockitic gneiss of massif G.

Gp: pyroxene granulite (YG 59).
Gi: intermediate pyroxene gneiss (YG 61).
Ga: augen gneiss (YG 62).
Ch: acid charnockite (YG 63).

Table 1. *Petrographic properties of constituents of pyroxene-biotite gneiss (YA 229, YA 303).*

| Pyroxene | | Mica | Feldspar | |
Rhombic	Monoclinic		K-feldspar	Plagioclase
rarely found.	0.2 mm in diameter, 1.0 mm as poikilo-blast including. bi, k-feld, pl grains. $2V_z = 60° - 57°$, $71° - 47°$, $\widehat{Zc} = 39° - 32°$, $38° - 34°$, alters to hornblende.	biotite, 0.2 mm in length, X-pale yellow brown, Y-brown, Z-reddish brown.	anhedral, 0.5 mm in size, hair perthite, porphyroblast (0.5 mm) with Carlsbad twin in some cases.	1.0 mm in size, polysynthetic twin, An 23.

Table 2. *Petrographic properties of constituents of enderbitic gneiss (YA 285).*

| Pyroxene | | Mica | Feldspar | |
Rhombic	Monoclinic		K-feldspar	Plagioclase
0.2-1.0 mm in size, $2V_x = 60° - 48°$, $N_x = 1.716$, $N_y = 1.725$, $N_z = 1.733$.	0.2-1.0 mm in size, $2V_z = 60° - 45°$, $\widehat{Zc} = 51° - 39°$, $N_z = 1.723$, alters to green hornblende.	biotite, 0.5 mm in size, X-pale yellow, Y-brown, Z-reddish brown, $N_z = 1.667$.	minor in amount, 1.0 mm in size, with hair perthite, small plagioclase inclusions.	most abundant, 0.5-1.0 mm in size, 0.5 mm in max., polysynthetic twin, antiperthite, An 25-33, inclusion in k-feldspar: An 28 ± fine plagioclase: An 25 ±.

Table 1. *Petrographic properties of constituents of pyroxene-biotite gneiss (YA 229, YA 303).*

	Mica	Feldspar		Quartz	Others
		K-feldspar	Plagioclase		
er, 1.0	biotite,	anhedral,	1.0 mm in size,	minor amount,	myrmekite,
·last	0.2 mm in length,	0.5 mm in size,	polysynthetic twin,	undulatory	hornblende,
-feld,	X-pale yellow brown,	hair perthite,	An 23.	extinction.	apatite,
	Y-brown,	porphyroblast (0.5 mm)			zircon,
	Z-reddish brown.	with Carlsbad twin			opaques.
		in some cases.			
de.					

Table 2. *Petrographic properties of constituents of enderbitic gneiss (YA 285).*

	Mica	Feldspar		Quartz	Others
		K-feldspar	Plagioclase		
e,	biotite,	minor in amount,	most abundant,	1.0-4.0 mm	myrmekite,
	0.5 mm in size,	1.0 mm in size,	0.5-1.0 mm in size,	in size,	apatite,
	X-pale yellow,	with hair perthite,	0.5 mm in max.,	intergranular.	opaques.
	Y-brown,	small plagioclase	polysynthetic twin,		
	Z-reddish brown,	inclusions.	antiperthite,		
	$N_z = 1.667$.		An 25-33,		
			inclusion in		
			k-feldspar: An 28 ±,		
			fine plagioclase: An		
			25 ±.		

Table 3. Petrographic properties of constituents of charnockitic gneiss.

| | Pyroxene | | Mica | Feldspar | |
	Rhombic	Monoclinic		K-feldspar	Plagioclase
Augen gneiss (YG 62)	0. 2 mm in size, $2V_x = 58° - 40°$, $2V_x = 52°$ in fine part, 47° in coarse part, $N_z = 1.731$.	0. 1-0. 5 mm in size, 2. 0 mm in max., $2V_z = 58° - 50°$, $\widehat{Zc} = 44° - 36°$, $2V_z = 50°$ in fine part, 55° in coarse part, $N_z = 1.723$	biotite, 1. 0 mm in length, X-pale yellow, Y-light brown, Z-reddish brown, $N_z = 1.655$.	1. 0-2. 0 mm in size, porphyroblast, (10. 0-20. 0 mm) in augen gneiss, hair perthite.	less abundant, 0. 5 mm in size, feeble albite twin, An 24, inclusions in k-feldspar : An l
Charnockite (YG 63)	1. 0 mm in size, $2V_x = 52° - 42°$, $N_z = 1.726$.	1. 0 mm in size $2V_z = 59° - 52°$, $\widehat{Zc} = 44° - 31°$, $N_z = 1.723$.	biotite, 1. 0 mm in length, X-pale yellow, Y-light brown, Z-reddish brown, $N_z = 1.660$.	1. 0 mm in size, 10. 0-40. 0 mm in porphyroblast, including pyroxenes and plagioclase, hair perthite and microperthite, undulatory extinction.	less abundant, 0. 2 mm in size, feeble albite twin, An 23-14, fine grain : An 16, inclusions in k-feldspar : An 2

Table 3. Petrographic properties of constituents of charnockitic gneiss.

| Monoclinic | Mica | Feldspar | | Quartz | Others |
		K-feldspar	Plagioclase		
5 mm in size, a in max., 8°−50°, °−36°, 0° in fine part, n coarse part, 723	biotite, 1.0 mm in length, X−pale yellow, Y−light brown, Z−reddish brown, $N_z = 1.655$.	1.0−2.0 mm in size, porphyroblast, (10.0− 20.0 mm) in augen gneiss, hair perthite.	less abundant, 0.5 mm in size, feeble albite twin, An 24, inclusions in k-feldspar : An 18.	0.5−1.0 mm in s·ze, undulatory extinction.	opaques, hornblende, apatite.

n in size
9°−52°,
°−31°,
723.
	biotite,
	1.0 mm in length,
	X−pale yellow,
	Y−light brown,
	Z−reddish brown,
	$N_z = 1.660$.
		1.0 mm in size,
		10.0−40.0 mm in
		  porphyroblast,
		  including pyroxenes
		  and plagioclase,
		hair perthite and
		  microperthite,
		undulatory extinction.
			less abundant,
			0.2 mm in size,
			feeble albite twin,
			An 23−14,
			fine grain : An 16,
			inclusions in
			    k-feldspar : An 23.
				0.5−2.0 mm in
				size,
				undulatory
				extinction.
					opaques,
					myrmekite,
					apatite.

petrographic properties are shown in Table 2.

Charnockitic gneisses are found in massif G. These gneisses are characterized by a banded structure manifested by regularly alternating aplitic and basic layers. The aplitic layers are stained reddish brown and have a faint foliation. They are composed of potassium-feldspar, quartz, plagioclase, orthopyroxene, clinopyroxene and biotite. The basic layers are dark grey and show a distinct preferred orientation of mafic minerals such as biotite and pyroxene. These layers are composed of monoclinic and rhombic pyroxene, biotite, and plagioclase. The aplitic and basic layers are mixed together forming a more or less intermediate gneiss, some of which shows a porphyritic augen texture resulting from potassium-feldspar porphyroblasts. There is a fairly continuous series from basic charnockite to acid charnockite, showing a gradual increase in the amount of potassium-feldspar as well as in the grain size and Fe/Mg ratio, as determined by the refractive indices of mafic minerals (Table 4 and Fig. 5). The light grey aplitic granites are characterized by purple-grey quartz grains. and are emplaced concordantly in the gneisses (Table 3).

Table 4. Optical properties of the constituents in the charnockitic gneisses from the massif G.

Rocks	Biotite N_z	Clino-pyroxene N_z	Ortho-pyroxene N_z	Plagioclase An %	Average grain size (mm)
Metabasite band (YG 59)	1.624	1.704	1.710	25	0.5 without potash-feldspar
Intermediate gneiss (YG 61)	1.646	1.716	1.720	n. d.	0.5 with potash-feldspar : 1.0-2.0
Augen gneiss (YG 62)	1.655	1.723	1.731	25-18	0.2-1.0 with potash-feldspar : 10.0-20.0
Aplitic band (YG 63)	1.666	1.723	1.726	23-14	1.0 with potash-feldspar : 10.0-40.0

b) Pyroxene syenites

The pyroxene syenite is divided into two species; porphyritic pyroxene syenite and pyroxene syenite. The porphyritic pyroxene syenite occurs in the eastern half of massif C and constitutes the major portions of massifs E and F. The dark color of the syenite is due to brownish-grey feldspars, the rock is foliated in some places. The syenites are characterized by oligoclase or potassium-feldspar porphyroblasts, both of which give blue schillerization owing to the presence of numerous oriented inclusions of magnetite (SHIBUYA and KIZAKI, in press). Some of these porphyroblasts are aggregates of smaller grains. In general, potassium-feldspars are rimed by small granular acidic plagioclase grains with myrmekites (Fig. 6). The rocks are composed of potassium-feldspar, biotite, mono-
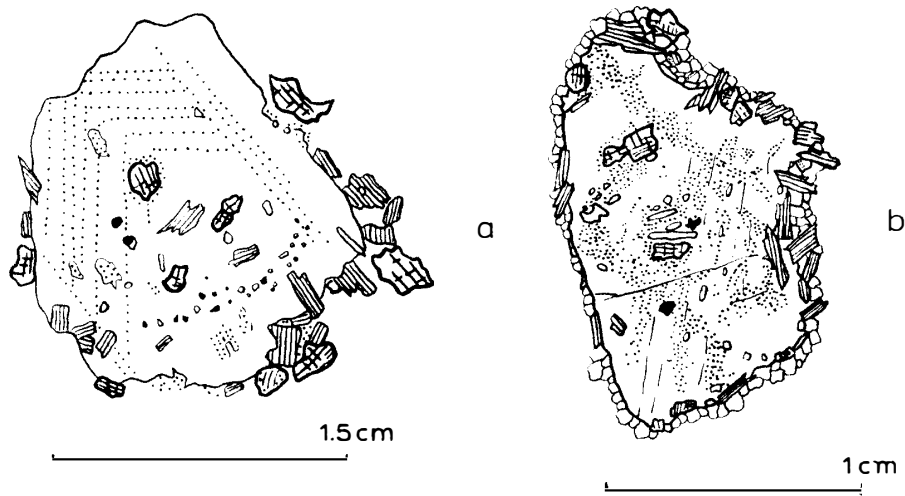
Fig. 6.   Oligoclase (a) and potassium-feldspar (b) porphyroblast in porphyritic pyroxene syenite.

clinic and rhombic pyroxene and plagioclase. Their petrographic properties are shown in Table 5. Only very few oligoclase porphyroblast-bearing pyroxene syenites are found, whereas potassium-feldspar porphyroblast-bearing rocks occupy the greater part of the porphyritic pyroxene syenite area. In these cases where the porphyroblasts are small (10.0 mm), the matrix of biotite, pyroxene and quartz is fine-grained (about 0.2 mm), with a preferred orientation, and post-kinematic pyroxenes attaining 2.0 mm, are observed (Fig. 7). As the potassium-feldspar porphyroblasts grow, to a maximum of about 20.0 mm, the associated minerals also increase in grain size to 1.0-1.5 mm.
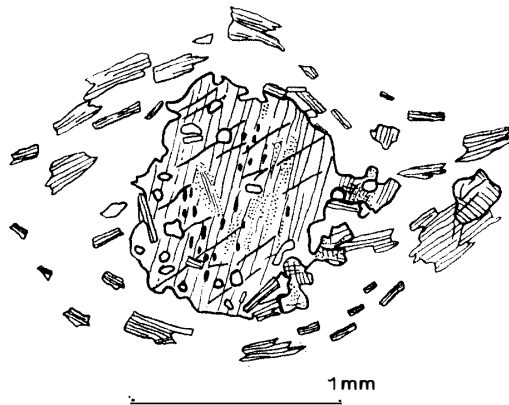

Fig. 7.   Post-kinematic growth of orthopyroxene in porphyritic
pyroxene syenite.

Pyroxene syenites are found in the eastern part of massif A and in parts of massifs E and F. These dark grey rocks are generally medium-grained, and the constituents show a preferred orientation. In massif A, these syenites include a great many angular fragments of amphibolites, enderbitic gneisses, pyroxene-

Table 5. *Petrographic properties of constituents of porphyritic pyroxene syenite.*

| | Pyroxene | | Mica | Feldspar | | Quartz | Others |
	Rhombic	Monoclinic		K-feldspar	Plagioclase		
Oligoclase porphyritic Pyroxene syenite (YC 231)	1.0 mm in size, $2V_x=56°$, $N_z=1.723$.	1.0 mm in size, lamellar extinction, $2V_z=58°-56°$, $\widehat{Zc}=52°-39°$, $N_z=1.710$.	biotite, 0.5 mm in length, lath shape, X-pale, yell. brown, Y-brownish khaki, Z-vandyke brown, $N_z=1.652$.	microcline perthite, 0.8 mm in size.	0.5 mm in matrix, 10.0 mm in porphyroblast, antiperthite including px, bi, h'bl, q grains, An 22-14, polysynthetic twin.	0.3 mm in size, undulatory extinction,	sphene, apatite, opaques.
Potash-feldspar porphyritic Pyroxene syenite (YC 239)	1.0-1.5 mm in size, $2V_x=47°-44°$, $N_z=1.719$, partially alters to green h'bl.	1.0-1.5 mm in size, lamellar extinction, $2V_z=56°-54°$, $\widehat{Zc}=41°-34°$, $N_z=1.709$, partially alters to green h'bl.	biotite, 1.0 mm in length, X-pale brownish yellow, Y-yellowish brown, Z-reddish brown, $N_z=1.641$.	hair perthite, 5.0-20.0 mm, porphyroblast including bi, pl, h'bl, px, ap grains, showing schiller phenomenon.	0.2 mm in size, minor amount, An 26-22.	0.3 mm in size, minor amount,	hornblende, zircon, apatite, opaques.

Table 6. *Petrographic properties of constituents of pyroxene syenite (YA 301).*

| Pyroxene | | Mica | Amphibole | Feldspar | | Others |
Rhombic	Monoclinic			K-feldspar	Plagioclase	
0.5-1.0 mm in size, round grain, usually alters to h'bl or bi,	0.5-1.0 mm in size, round grain, usually alters to h'bl or bi,	biotite, 1.0 mm in length, X-pale yell. brown, Y-pale brown,	hornblende, 1.0 mm in size, X-almost colorless, Y-pale br. green,	2.0 mm in length, 5.0 mm in max., Carlsbad twin, hair perthite.	1.5 mm in size, polysynthetic twin, antiperthite, An 27-21.	quartz, myrmekite, apatite, zircon,

Potash-feldspar porphyritic pyroxene syenite (YC 239)						
1.0–1.5 mm in size, $2V_x=47°-44°$, $N_z=1.719$, partially alters to green h'bl.	1.0–1.5 mm in size, lamellar extinction, $2V_z=56°-54°$, $\widehat{Zc}=41°-34°$, $N_z=1.709$, partially alters to green h'bl.	biotite, 1.0 mm in length, X–pale brownish yellow, Y–yellowish brown, Z–reddish brown, $N_z=1.641$.	hair perthite, 5.0–20.0 mm, porphyroblast including bi, pl, h'bl, px, ap grains, showing schiller phenomenon.	0.2 mm in size, minor amount, An 26–22.	0.3 mm in size, minor amount,	hornblende, zircon, apatite, opaques.

Table 6. Petrographic properties of constituents of pyroxene syenite (YA 301).

Pyroxene		Mica	Amphibole	Feldspar		Others
Rhombic	Monoclinic			K-feldspar	Plagioclase	
0.5–1.0 mm in size, round grain, usually alters to h'bl or bi, sometimes polygonized to fine grains (0.1 mm), $2V_x=51°-49°$, $N_x=1.705$, $N_y=1.713$, $N_z=1.721$.	0.5–1.0 mm in size, round grain, usually alters to h'bl or bi, sometimes polygonized to fine grains (0.1mm), $2V_z=62°-46°$, $\widehat{Zc}=5°-36°$, $N_z=1.723$.	biotite, 1.0 mm in length, X–pale yell. brown, Y–pale brown, Z–reddish brown, $N_z=1.666$.	hornblende, 1.0 mm in size, X–almost colorless, Y–pale br. green, Z–green, $2V_x=80°-71°$, $\widehat{Zc}=2°-11°$, $N_z=1.673$, shows poikilitic overgrowth on pyroxenes, including pyroxene relics.	2.0 mm in length, 5.0 mm in max., Carlsbad twin, hair perthite.	1.5 mm in size, polysynthetic twin, antiperthite, An 27–21.	quartz, myrmekite, apatite, zircon, opaques.

biotite gneisses, and they also contain basic schlieren, so that they are nebulitic and agmatitic in appearance. It is not known whether the migmatitic pyroxene syenite was formed by migmatization-syenitization of the pyroxene gneisses or by synkinematic intrusion of syenite. These rocks are traversed by aplite intrusions one to several meters wide. In massifs E and F, the syenite gradually grades from porphyritic pyroxene syenite into pink microcline granite without any distinct boundary. This represents a kind of static granitization of porphyritic pyroxene syenite into microcline granite.

These rocks are composed of potassium-feldspar, biotite, clinopyroxene and orthopyroxene with lesser amounts of plagioclase, quartz and green hornblende. The petrographic properties of these minerals are shown in Table 6. Microscopically, the pyroxene is usually altered to green hornblende and/or biotite, and the potassium-feldspar is in a somewhat elongated euhedral form with Carlsbad twinning. Even the microcline granite of the area contains relict pyroxene and uralitic hornblende.

c) *Migmatitic gneiss and biotite granite*

Migmatitic gneisses are found on the southwestern ridge of massif D. These gneisses are medium-grained, showing a preferred orientation of minerals and inclusions, and are characterized by the same kind of purple grey quartz crystals

Table 7. Petrographic properties of constituents of migmatitic gneiss and biotite granite.

| | Mica | Feldspar | | Quartz | Others |
		K-feldspar	Plagioclase		
Migmatitic gneiss (YD 324)	biotite, 0. 5 mm in length, X-pale yellow, Y-yellow ochre, Z-khaki brown, partially alters to chlorite.	microcline perthite, 1. 0-2. 0 mm.	1. 0-2. 0 mm in size, polysynthetic twin, antiperthite, An 30.	1. 0-2. 0mm in size.	zoisite, apatite, zircon, sphene, opaques, myrmekite.
Biotite granite (YD 337)	biotite, 1. 0 mm in length, Z-pale br. yellow, Y-pale brown, Z-reddish brown.	microline and orthoclase perthite, 1. 0-2. 0 mm in size.	0. 5-1. 5 mm in size, polysynthetic twin, antiperthite, An 30-22.	1. 0-2. 0mm in size.	apatite, zircon, opaques, sericite, myrmekite.
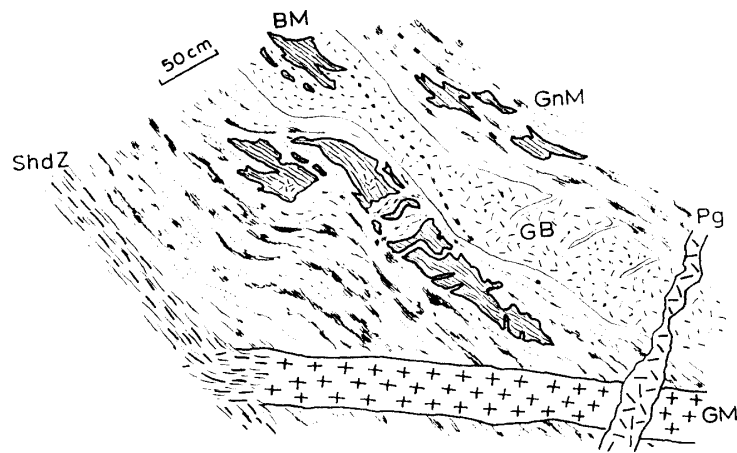
*Fig. 8. Migmatitic gneiss (GnM) and biotite granite (GB) with metabasite
inclusions (BM) are traversed by microcline granite dike (GM) which
are sheared by thrust movement (ShdZ). Pegmatite (Pg) is a product
of the last emplacement.*

as seen in the biotite granites. The rocks are heterogeneous, having many inclusions of pyroxene amphibolite, basic granulite and basic schlieren which range in size from several centimeters to several decimeters. Disintegration of the basic layers into stringers and streaks is observed, and the rocks resemble the agmatitic and nebulitic gneisses. Around the rims of these paleosomes and schlieren, there are concentrations of pyroxenes, especially orthopyroxene, which suggest a kind of basic front resulting from migmatization. There have been subsequent intrusions of basic dikes, pink microcline granite sheets and pink pegmatite successively into the gneisses (Fig. 8). These basic dikes have metamorphosed amphibolite.

These rocks have been affected by a thrust movement. The gneisses, microcline granite and amphibolite are sheared as well as granulated, and the gneisses mix with microcline granite sheets along the shear zones (Fig. 8).

Massive biotite granites occur in the gneiss as concordant sheet-like bodies which may have been granitized from migmatitic gneiss. Biotite granite dikes having the same characteristics traverse the gneisses and granites. This indicates anatexitic mobilization of the biotite granite, a kind of SEDERHOLM effect (ESKOLA, 1963), though no metabasites are traversed. These gneisses and granites are petrographically similar as is shown in Table 7.

Molybdenite impregnation is seen in some places in the migmatitic gneisses and biotite granites. The minerals are usually concentrated along the shear zones as well as around the basic inclusions in these rocks.

d) Granitic gneiss

Granitic gneisses occur in massif B, in the western half of massif C, and in the eastern part of massif D. The gneisses are medium-to coarse-grained and pinkish grey in color, with distinct gneissosity. Massif B is banded and porphyritic (augen structure), while massifs C and D are predominantly nebulitic in general.

The banded structure is not distinct, but alternation of mafic and felsic layers,

2 to 5 mm thick, is observed. Porphyroblasts of potassium-feldspar are scattered in some parts of the banded gneiss, which is frequently intruded by granite sheets.

These pink granite sheets, which vary from fine-grained, massive granite to coarse, pegmatitic granite, alternate concordantly with augen gneisses 50–100 cm thick, resembling in appearence an arteritic migmatite. The granites, however, may not have been intrusives but may have developed *in situ* as a result of the influx of granitic solution, as many relicts of the gneiss in the granite sheets preserve their original orientation.

Subsequently, basic dikes were intruded into these rocks, and then pegmatites were intruded obliquely to the gneisses.

The gneisses are composed primarily of microcline, plagioclase, quartz, biotite and hornblende, whose properties are shown in Table 8. Their composition varies more or less toward the northern area; toward massifs C and D, where clinopyroxenes are sometimes found as relict mineral. The clinopyroxenes are bluish green in thin section and have strong pleochroism. The potassium-feldspar in the northern area is orthoclase with flame-like perthite, instead of the microcline usually found in the gneisses of the southern area. The refractive indices of hornblende and biotite increase from north to south in the gneisses, approaching those of the same minerals in the microcline granite.

e) *Microcline granite*

Microcline granite occurs in massifs B, C, D and E. It is emplaced as rather small sheets and stocks, associated with the granitic gneiss and the microcline pegmatite. The granite is pink, usually medium to coarse-grained, and massive. It is composed mainly of potassium-feldspar, quartz and plagioclase, with minor amounts of hornblende and biotite (Table 9).

The granite in massif E is somewhat different. The pyroxene syenite grades into the microcline granite. This rock contains some perthite, less microcline, uralitic hornblende, and fewer relicts of pyroxene which are altered to hornblende, biotite and chlorite. Scapolite-bearing microcline granites are sometimes found in this massif. Scapolite occurs in the pegmatitic part of the granite adjoining the metabasite, as radial aggregates including elongated crystals several centimeters long.

f) *Metabasites*

Metabasites are variable in their occurrence as well as in their petrography. There are metamorphosed basic layers concordant to the foliation of the country rocks, and metamorphosed, cross-cutting basic dikes. These rocks are classified into three rock species; basic granulite, pyroxene amphibolite and biotite amphibolite (Table 10).

Basic granulite occurs as lenticular, basic bands and inclusions in the pyroxene syenites of massifs A and E. The rocks are dark grey and rather fine-grained, with the constituents showing a preferred orientation. They are composed mainly of fine-grained pyroxene, biotite, and potassium-feldspar.

Pyroxene amphibolites are found as basic inclusions in pyroxene gneiss, por-

Table 8. Petrographic properties of constituents of granitic gneiss.

	Mica	Amphibole	Feldspar		Quartz	Others
			K-feldspar	Plagioclase		
Augen gneiss (YB 262)	biotite, 1.0 mm in length, X-yellow ochre, Y-khaki, Z-dark russet brown, $N_z=1.660$, muscovite, minor in amount.	hornblende, minor in amount, 0.5 mm in size, X-greenish yellow, Y-yellow. green, Z-bluish green, $2V_x=66°-56°$, $\widehat{Z}c=7°-3°$, $N_z=1.709$.	microcline, 10.0-20.0 mm in size, surrounded by small grains of plagioclase, quartz and microcline.	0.5-2.0mm in size, polysynthetic twin, An 29-22; An 22 in average.	1.0-2.0 mm in size.	apatite, zircon, sphene, opaques, myrmekite.
Nebulitic gneiss (YC 310)	biotite, 1.0 mm in length X-pale yellow, Y-pale brown, Z-light brown, $N_z=1.656$.	hornblende, minor in amount, 0.5 mm in size, X-pale br. green, Y-brownish green, Z-bluish green, $2V_x=72°-56°$, $\widehat{Z}c=21°-13°$, $N_z=1.691$, pseudomorph. of pyroxene.	microcline, microcline perthite, 1.0-4.0 mm in size.	0.5-2.0mm in size, polysynthetie twin, An 28-6; An 18 in average.	1.0-2.0mm in size.	sphene, apatite, zircon, opaques.

Table 9. *Petrographic properties of constituents of microcline granite* (YC 313).

Mica	Amphibole	Feldspar		Quartz	Others
		K-feldspar	Plagioclase		
biotite,	hornblende,	microcline perthite,	1.0–2.0 mm in size,	1.0–2.0 mm in size,	zircon,
0.5 mm in length,	0.5 mm in size,	1.0–2.0 mm in size,	polysynthetic twin,	undulatory extinction.	apatite,
X-pale br. yellow,	X-brownish green,		An 28–13,		opaques,
Y-pale brown,	Y-brownish green,		sericitized.		chlorite,
Z-reddish brown,	Z-bluish green,				$No = 1.556$,
$N_z = 1.660$,	partially chloritized.				scapolite
partially chloritized.					$Ne = 1.544$.

phyritic syenite, and migmatitic gneiss. The rocks are dark in appearence and generally fine-grained, but include coarser portions. It is thought that the rocks were originally biotite amphibolite, because clinopyroxene and orthopyroxene occur only at the margin of the inclusions and in coarser veinlets derived from the country rock. The pyroxenes more or less represent porphyroblasts, and have included flakes of biotite and hornblende.

Biotite amphibolites usually occur in the granitic gneiss, excepting that of massif D where it contains clinopyroxene and a small amount of orthopyroxene. The rocks are generally modified by granitization, as is evidenced by the metablastesis of potassium-feldspar and metatexis due to the invasion of granite and pegmatite veins.

Basic dikes cross-cutting the country rocks are metamorphosed into metabasites, showing a prefered orientation parallel to the dike boundaries. They are composed of biotite, clinopyroxene, hornblende, plagioclase, potassium-feldspar and quartz, not only in the pyroxene syenite but also in the migmatitic gneiss and granitic gneiss of massif C (Figs. 9 and 10). However, the dikes in the
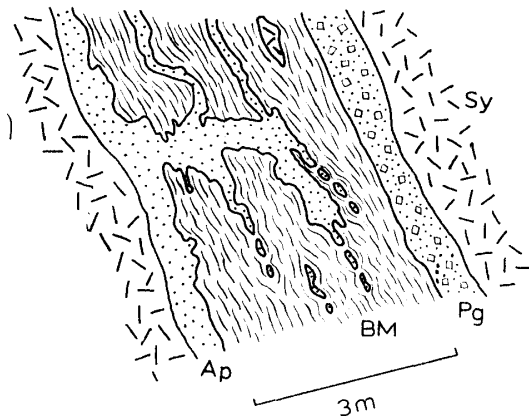
Fig. 9. Basic dike (BM) intruded by subsequent aplite (Ap) and pegmatite (Pg) is metamorphosed to basic granulite, while the aplite veins are boudinaged in pyroxene syenite of massif C.
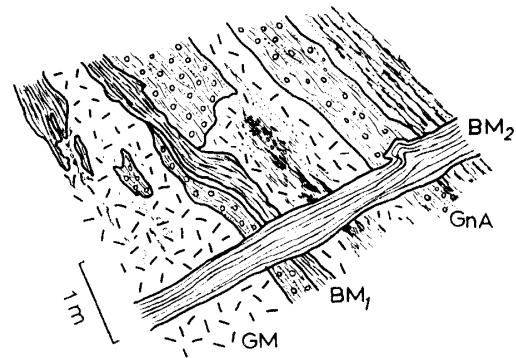
Fig. 10. Microcline granite (GM), granitic gneiss, augen gneiss (GnA) and intercalated metabasite layer (biotite amphibolite) (BM₁) are traversed by metabasite dike (pyroxene amphibolite) (BM₂) in massif C.

granite gneiss of massif B are biotite amphibolite without pyroxenes. These dikes are 50 cm to 3 m wide, and well-defined.

The mineral assemblages of the metabasite layers as well as those of the meta-dikes correspond generally to those of the country rocks. It is clear that the mineral assemblages of the meta-dikes reflect the P-T conditions during the recrystallization of granite gneiss of massif B, and of granite gneiss and pyroxene syenite of the other massifs.

These metabasite layers and meta-dikes are usually associated with pink pegmatites.

Table 10. Petrographic properties of constituents of metabas

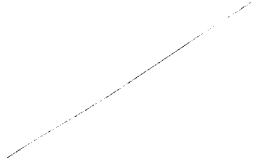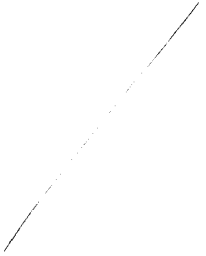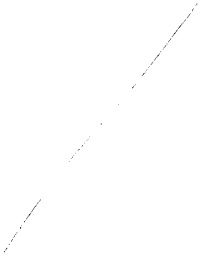| | Pyroxene | | Amphibole | Mica | |
	Rhombic	Monoclinic			
Basic granulite (YE 52)	0.5-1.0 mm in size, $2V_x = 58°-43°$, $N_z = 1.712$.	0.5-1.0mm in size, $2V_z = 65°-43°$, $\widehat{Zc} = 44°-33°$, $N_z = 1.714$.		biotite, 1.0mm in length, X-pale yellow, Y-brownish yellow, Z-khaki brown, $N_z = 1.624$.	0.3 hai un
Pyroxene amphibolite (YA 282)	0.5-1.0 mm in size, $2V_x = 40°-58°$, $N_z = 1.734$.	0.5-1.0 mm in size, $2V_z = 78°-49°$, $\widehat{Zc} = 59°-24°$, $N_z = 1.722$.	hornblende, 1.0-2.0 mm in length, X-pale gr. yellow, Y-yellowish green, Z-brownish green, $2V_x = 83°-78°$, $\widehat{Zc} = 17°-14°$.	biotite, 0.5-1.0 mm in size, X-pale br. yellow, Y-reddish brown, Z-dark red. brown, $N_z = 1.671$.	
Biotite amphibolite (YB 272)			hornblende, 1.0 mm in size, sieve structure, X-pale green, Y-yellowish green, Z-bluish green, $2V_x = 65°-53°$, $\widehat{Zc} = 27°-12°$, $N_z = 1.698$.	biotite, 1.0 mm in length, X-pale yellowish ochre, Y-greenish brown, Z-russet brown, $N_z = 1.627$.	mi 1.0
Metabasite dike (YC 232)		0.5 mm in size, $2V_z = 58°-50°$, $\widehat{Zc} = 39°-30°$, $N_z = 1.708$.		biotite, 0.5 mm in length, X-pale yellow, Y-brown, Z-reddish brown, $N_z = 1.664$.	
Metabasite dike (YC 318)		0.5 mm in size, $2V_z = 64°-54°$, $\widehat{Zc} = 46°-31°$. $N_z = 1.710$.	minor in amount, pale green hornblende alters from pyroxene.	biotite, 1.0 mm in length, X-pale yellow, Y-brown, Z-vandyke brown, $N_z = 1.638$	mi 0.5

ble 10. *Petrographic properties of constituents of metabasites.*

Amphibole	Mica	Feldspar		Others
		K-feldspar	Plagioclase	
	biotite, 1.0mm in length, X-pale yellow, Y-brownish yellow, Z-khaki brown, $N_z = 1.624$.	0.3-0.1 mm in size, hairperthite, undulatory extinction.	rarely occur, 0.3mm in size, An 23.	apatite, zircon, opaques.
ıde, nm in length, gr. yellow, vish green, ıish green, ;°-78°, -14°.	biotite, 0.5-1.0 mm in size, X-pale br. yellow, Y-reddish brown, Z-dark red. brown, $N_z = 1.671$.		0.5 mm in size, polysynthetic twin, An 51-34.	zircon, apatite, opaques, quartz, k-feldspar.
ıde, in size, ucture, green, vish green, green, ;°-53°, -12°, 98.	biotite, 1.0 mm in length, X-pale yellowish ochre, Y-greenish brown, Z-russet brown, $N_z = 1.627$.	microcline perthite, 1.0 mm in size.	minor in amount, 0.5 mm in size, polysynthetic twin, An 27-21.	myrmekite, apatite, sphene, zircon, quartz.
	biotite, 0.5 mm in length, X-pale yellow, Y-brown, Z-reddish brown, $N_z = 1.664$.		0.5 mm in size, faint polysynthetic twin, undulatory extintion, An 22-9.	apatite, sphene, zircon sericite, quartz
n amount, een hornblende from pyroxene.	biotite, 1.0 mm in length, X-pale yellow, Y-brown, Z-vandyke brown, $N_z = 1.638$	microcline perthite, 0.5 mm in size.	0.5 mm in size, faint polysynthetic twin, An 26-14.	apatite, sphene, zircon, quartz.
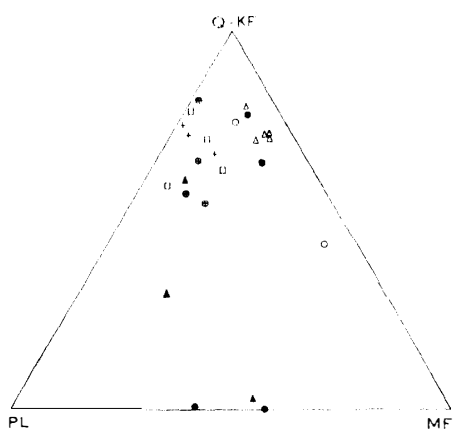
Fig. 11. Modal relation in Q·Kf-Pl-Mf
diagram. Legend is shown in Fig 13.
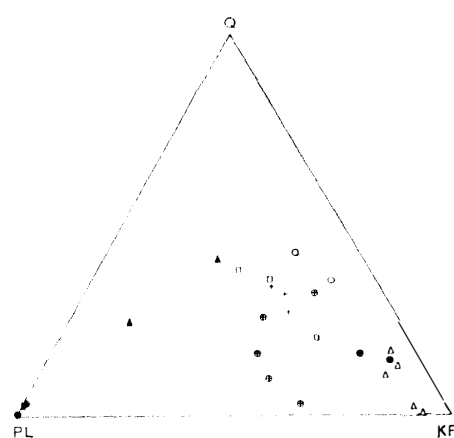
Fig. 12. Modal relation in Q-Pl-Kf dia-
gram.

Modal relations

The modal relation in the Q · Kf-Pl-Mf and Q-Pl-Kf diagrams are shown in Figs. 11 and 12. The compositional fields of the charnockitic group and granitic group are separated from each other in these diagrams. The granite gneiss has a general tendency to increase quartz and potassium-feldspar, approaching to the composition of the granitic group, while the charnockitic group is separated into pyroxene syenite rich in potassium-feldspar and enderbitic pyroxene gneiss with less potassium-feldspar. It is, however, evident that the enderbitic
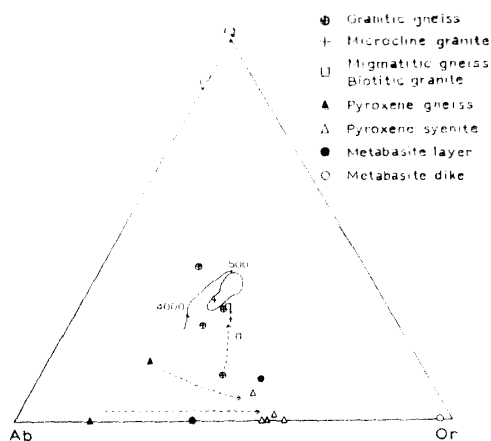
Fig. 13. Normative Q-Ab-Or diagram. The
closed contour corresponds to the highest
concentration of the granitic rocks plotted
on this diagram. The line 500-4,000
indicates the trend of the position of
the lowest-crystallizing composition with
H_2O pressure from 500 atm to 4,000
atm. Broken lines with arrows represent
the succession of the formation of rocks
as reduced from the field observation.
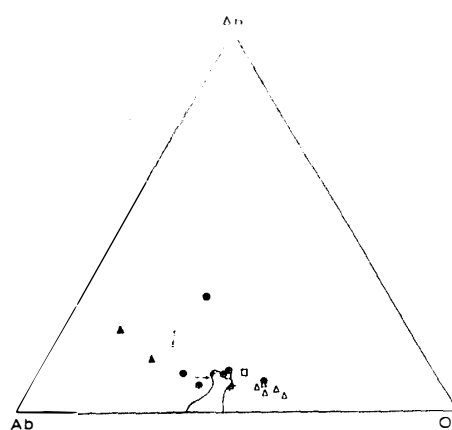
Fig. 14. Normative An-Ab-Or diagram.

pyroxene gneiss grades into the pyroxene syenite with increasing potassium-feldspar.

Petrochemistry

Bulk chemical compositions of 20 rocks are presented in Table 11, together with C. I. P. W. molecular norms. The Q-Ab-Or and An-Ab-Or diagrams are shown in Figs. 13 and 14. In these diagrams as in the modal diagrams, the charnockitic group is distinct from the granitic rock group. The granitic group shows a distinct trend to cluster in the eutectoid field (TUTTLE and BOWEN, 1958) because of the enrichment of Q and/or Or from the granite gneiss to the granite. This trend may indicate granitization. Consequently, a palingenetic rheomorphism may be expected in this field, related to the SEDERHOLM effect, as stated above. The difference between pyroxene gneiss and pyroxene syenite is represented by the enrichment of Or in the latter as shown in both diagrams. In the Ca-Mg-Fe diagram, the two groups are also distinctly separated (Fig. 15). It is, therefore, evident from petrological point of view that these two rock groups belong originally to different units.

Fig. 15. Ca-Mg-Fe diagram.

Table 11. *Modal and chemical compositions of rocks from the Yamato Sanmyaku, E...*

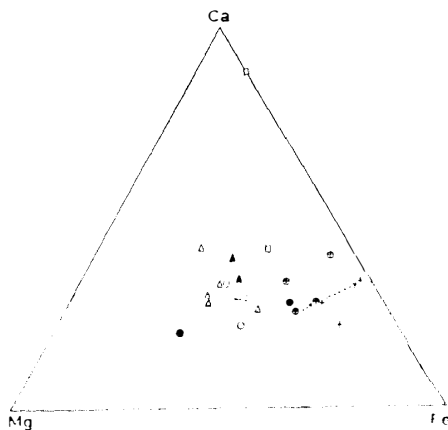|	YA303	YA285	YE54	YC238	YA292	YA301	YF87	YD320	YD335	YC310	YD224	YB261	YB27
Mode, volume per cent													
Quartz	33.0	19.0	0.9	6.5	10.2	4.4	0.9	20.6	15.7	11.8	27.9	5.4	17.
Potash-feldspar	23.4	11.4	71.4	61.9	58.7	64.0	77.0	44.4	52.9	41.1	51.3	48.1	45.
Plagioclase	33.8	48.4	4.9	7.9	7.4	11.1	6.9	29.6	21.5	32.4	18.6	28.5	27.
Biotite	6.9	9.1	10.3	16.0	8.3	10.0	2.0	3.5	8.5	8.3	0.2	6.4	3.
Hornblende	2.0	—	—	—	13.2	2.9	—	0.4	—	2.5	1.5	8.7	6.
Clinopyroxene	0.4	8.3	9.5	5.9	0.1	5.7	11.3	—	—	—	—	—	-
Orthopyroxene	—	2.7	1.4	1.4	0.1	0.4	0.4	—	—	—	—	—	-
Apatite	0.2	0.3	0.9	0.4	0.8	0.3	0.8	0.2	0.3	0.3	tr	0.5	0.
Zircon	—	0.1	—	—	—	0.1	tr	tr	tr	0.1	tr	0.2	t
Sphene	—	—	—	—	—	—	—	tr	tr	0.8	tr	0.1	0.
Opaque	0.1	0.2	0.3	0.2	1.3	0.1	0.7	0.2	0.9	1.5	tr	0.9	0.
Others*	0.4	0.6	0.5	0.1	—	1.0	—	1.1	0.1	1.1	0.7	1.3	-
Total	100.2	100.1	100.1	100.3	100.1	100.0	100.0	100.0	99.9	99.9	100.2	100.1	100.
Chemical compositions													
SiO_2	65.02	57.00	59.33	55.28	59.78	55.31	60.15	73.13	71.25	69.29	77.24	61.69	71.5
TiO_2	0.69	0.54	0.74	1.14	1.49	0.79	0.69	0.24	tr	0.64	0.14	1.39	0.5
Al_2O_3	15.74	17.92	15.63	13.00	14.49	11.60	14.54	13.78	15.84	13.53	11.96	14.86	13.3
Fe_2O_3	1.22	1.39	1.54	2.07	2.16	1.70	1.03	0.55	0.16	2.06	0.92	3.23	1.2
FeO	2.70	4.38	2.62	5.01	3.84	6.04	2.44	1.08	0.16	1.77	0.49	3.40	1.4
MnO	0.04	0.09	0.04	0.10	0.07	0.14	0.04	tr	tr	0.02	tr	0.07	0.0
MgO	2.22	3.41	3.22	6.18	2.74	6.54	3.63	0.55	tr	0.83	0.11	2.03	0.7
CaO	3.41	6.41	4.09	5.77	3.42	6.56	6.10	1.75	2.31	2.09	1.12	3.25	1.9
Na_2O	5.22	5.78	3.72	2.94	3.49	2.55	3.23	3.58	3.77	4.25	3.75	3.90	3.4
K_2O	3.11	1.80	7.37	5.97	6.47	6.13	7.22	4.99	6.13	4.39	3.34	5.29	4.9
P_2O_5	0.38	0.24	0.67	0.89	0.84	1.06	0.62	0.09	0.32	0.31	0.03	0.50	0.1
$H_2O(+)$	0.33	0.56	0.20	0.48	1.10	0.59	tr	0.14	tr	0.11	0.42	0.48	0.0
$H_2O(-)$	0.41	0.75	0.37	0.67	0.15	0.83	0.39	0.18	0.15	0.17	0.22	0.47	0.4
CO_2	0.16	0.28	0.22	0.20	0.02	0.46	0.19	0.06	0.15	0.34	0.26	tr	0.1
Total	100.65	100.55	99.76	99.70	100.06	100.20	100.27	100.12	100.24	99.80	100.09	100.56	99.9
$Mg/Mg+Fe''+Fe'''+Mn \times 100$													
	50.8	51.6	59.2	61.3	45.9	60.5	64.9	40.0	0.0	29.3	15.4	37.2	36.
C. I. P. W. (molecular) Norm													
q	7.5	—	—	—	5.3	—	0.8	26.9	20.4	21.1	37.8	9.8	26.
or	18.0	10.5	43.5	35.5	39.0	36.5	42.5	30.0	36.0	26.5	20.0	32.0	29.
ab	46.5	51.5	33.5	26.5	32.0	23.0	28.5	32.5	34.0	38.5	34.5	35.5	32.
an	10.3	17.5	4.0	4.8	4.5	2.3	3.8	6.5	8.3	5.0	6.3	7.3	6.
ol	—	4.8	2.1	6.0	—	9.6	—	—	—	—	—	—	-
hy	7.2	3.2	3.0	7.0	10.4	5.2	3.4	2.0	—	1.0	—	4.8	2.
di	3.2	10.0	10.0	14.4	5.2	19.2	17.6	0.8	—	3.2	—	4.4	1.
mt	1.2	1.4	1.7	2.3	2.2	1.8	1.1	0.6	0.2	2.3	1.1	3.3	1.
il	1.0	0.8	1.0	1.6	2.2	1.2	1.0	0.4	—	1.0	0.2	2.0	0.
ap	0.8	0.5	1.3	1.9	1.9	2.1	1.3	0.3	0.5	0.5	—	1.1	0.
ne	—	—	—	—	—	—	—	—	—	—	—	—	-

YA303 : Pyroxene-biotite gneiss from massif A.
YA285 : Enderbitic gneiss from massif A.
YE 54 : Pyroxene syenite from massif E.
YC238 : Py... ... pyroxene syenite from massif C.

YD224 : Granitic gneiss (nebulitic gneiss) from m...
YB261 : Granitic gneiss (augen gneiss) from mass...
YB278 : Granitic gneiss (augen gneiss) from mass...
YB265 : Microcline granite from massif B.

and chemical compositions of rocks from the Yamato Sanmyaku, East Antarctica.

	YF87	YD320	YD335	YC310	YD224	YB261	YB278	YB265	YC313	YD333	YG59	YC307	YB253	YC318
	0.9	20.6	15.7	11.8	27.9	5.4	17.0	24.2	31.3	26.7	—	11.0	6.7	16.2
	77.0	44.4	52.9	41.1	51.3	48.1	45.3	46.8	41.3	40.1	—	51.5	37.3	26.4
	6.9	29.6	21.5	32.4	18.6	28.5	27.3	24.1	23.2	21.1	45.2	9.9	41.9	6.8
	2.0	3.5	8.5	8.3	0.2	6.4	3.1	3.6	0.2	10.6	20.2	8.6	7.5	38.6
	—	0.4	—	2.5	1.5	8.7	6.6	—	—	0.8	—	15.0	4.1	—
	11.3	—	—	—	—	—	—	—	—	—	23.9	—	—	10.1
	0.4	—	—	—	—	—	—	—	—	—	10.1	—	—	—
	0.8	0.2	0.3	0.3	tr	0.5	0.1	0.5	tr	tr	tr	1.4	0.3	0.8
	tr	tr	tr	0.1	tr	0.2	tr	0.4	tr	tr	tr	0.3	0.1	tr
	—	tr	tr	0.8	tr	0.1	0.5	tr	tr	—	—	1.6	0.2	0.8
	0.7	0.2	0.9	1.5	tr	0.9	0.1	0.5	0.5	tr	tr	0.4	tr	tr
	—	1.1	0.1	1.1	0.7	1.3	—	0.4	1.2	0.7	0.6	0.3	1.8	—
	100.0	100.0	99.9	99.9	100.2	100.1	100.0	100.5	97.7	100.0	100.0	100.0	99.9	99.7
	60.15	73.13	71.25	69.29	77.24	61.69	71.51	72.06	71.63	70.80	50.82	59.19	52.02	50.18
	0.69	0.24	tr	0.64	0.14	1.39	0.54	0.44	0.24	0.64	0.89	1.43	1.54	1.30
	14.54	13.78	15.84	13.53	11.96	14.86	13.32	13.97	13.76	13.04	10.96	13.57	13.79	7.19
	1.03	0.55	0.16	2.06	0.92	3.23	1.23	1.12	1.39	1.10	1.45	3.62	2.32	6.91
	2.44	1.08	0.16	1.77	0.49	3.40	1.42	0.92	0.89	3.51	9.08	3.95	5.27	6.81
	0.04	tr	tr	0.02	tr	0.07	0.01	tr	tr	0.04	0.18	0.15	0.12	0.18
	3.63	0.55	tr	0.83	0.11	2.03	0.74	0.41	0.05	0.64	13.34	2.51	5.25	9.21
	6.10	1.75	2.31	2.09	1.12	3.25	1.93	1.13	1.36	1.52	8.07	4.44	6.91	7.48
	3.23	3.58	3.77	4.25	3.75	3.90	3.49	3.60	3.75	3.49	2.14	3.06	2.64	1.89
	7.22	4.99	6.13	4.39	3.34	5.29	4.92	5.36	5.51	4.20	2.27	6.20	6.31	6.50
	0.62	0.09	0.32	0.31	0.03	0.50	0.16	0.12	0.09	0.14	0.05	0.92	1.10	1.36
	tr	0.14	tr	0.11	0.42	0.48	0.08	tr	0.04	0.31	0.27	0.32	0.53	0.85
	0.39	0.18	0.15	0.17	0.22	0.47	0.42	0.66	0.38	0.27	0.38	0.25	0.94	0.24
	0.19	0.06	0.15	0.34	0.26	tr	0.13	0.03	0.37	0.18	0.11	tr	0.68	0.03
	100.27	100.12	100.24	99.80	100.09	100.56	99.90	99.82	99.46	99.88	100.01	99.61	99.42	100.13
	64.9	40.0	0.0	29.3	15.4	37.2	36.7	28.6	5.6	19.6	69.4	55.6	37.9	55.5
	0.8	26.9	20.4	21.1	37.8	9.8	26.1	26.5	25.1	27.2	—	8.2	—	—
	42.5	30.0	36.0	26.5	20.0	32.0	29.5	32.0	33.0	25.5	13.0	37.5	38.5	39.0
	28.5	32.5	34.0	38.5	34.5	35.5	32.0	33.0	34.5	32.0	19.0	28.0	24.5	—
	3.8	6.5	8.3	5.0	6.3	7.3	6.8	4.5	4.5	6.5	13.5	5.0	7.0	(ac) 13.2
	—	—	—	—	—	—	—	—	—	—	21.0	—	8.4	16.2
	3.4	2.0	—	1.0	—	4.8	2.2	—	(wo) 0.4	—	10.8	3.8	0.2	0.8
	17.6	0.8	—	3.2	—	4.4	1.2	—	0.4	—	20.0	9.2	16.4	23.2
	1.1	0.6	0.2	2.3	1.1	3.3	1.2	1.2	1.5	1.2	1.5	4.1	2.6	2.4
	1.0	0.4	—	1.0	0.2	2.0	0.8	0.6	0.4	1.0	1.2	2.4	2.2	1.8
	1.3	0.3	0.5	0.5	—	1.1	0.3	0.3	0.4	0.3	0.3	1.9	2.4	2.9
	—	—	—	—	—	—	—	—	0.3	—	—	—	—	0.6

YD224: Granitic gneiss (nebulitic gneiss) from massif D.
YB261: Granitic gneiss (augen gneiss) from massif B.
YB278: Granitic gneiss (augen gneiss) from massif B.

Hornblende	2.0				15.2	2.8		5.4			2.5	1.0	2.0
Clinopyroxene	0.4	8.3	9.5	5.9	0.1	5.7	11.3	—	—	—	—	—	—
Orthopyroxene	—	2.7	1.4	1.4	0.1	0.4	0.4	—	—	—	—	—
Apatite	0.2	0.3	0.9	0.4	0.8	0.3	0.8	0.2	0.3	0.3	tr	0.5
Zircon	—	0.1	—	—	—	0.1	tr	tr	tr	0.1	tr	0.2
Sphene	—	—	—	—	—	—	—	tr	tr	0.8	tr	0.1
Opaque	0.1	0.2	0.3	0.2	1.3	0.1	0.7	0.2	0.9	1.5	tr	0.9
Others*	0.4	0.6	0.5	0.1	—	1.0	—	1.1	0.1	1.1	0.7	1.3
Total	100.2	100.1	100.1	100.3	100.1	100.0	100.0	100.0	99.9	99.9	100.2	100.1	100

Chemical compositions

SiO_2	65.02	57.00	59.33	55.28	59.78	55.31	60.15	73.13	71.25	69.29	77.24	61.69	71.
TiO_2	0.69	0.54	0.74	1.14	1.49	0.79	0.69	0.24	tr	0.64	0.14	1.39	0.
Al_2O_3	15.74	17.92	15.63	13.00	14.49	11.60	14.54	13.78	15.84	13.53	11.96	14.86	13.
Fe_2O_3	1.22	1.39	1.54	2.07	2.16	1.70	1.03	0.55	0.16	2.06	0.92	3.23	1.
FeO	2.70	4.38	2.62	5.01	3.84	6.04	2.44	1.08	0.16	1.77	0.49	3.40	1.
MnO	0.04	0.09	0.04	0.10	0.07	0.14	0.04	tr	tr	0.02	tr	0.07	0.
MgO	2.22	3.41	3.22	6.18	2.74	6.54	3.63	0.55	tr	0.83	0.11	2.03	0.
CaO	3.41	6.41	4.09	5.77	3.42	6.56	6.10	1.75	2.31	2.09	1.12	3.25	1.
Na_2O	5.22	5.78	3.72	2.94	3.49	2.55	3.23	3.58	3.77	4.25	3.75	3.90	3.
K_2O	3.11	1.80	7.37	5.97	6.47	6.13	7.22	4.99	6.13	4.39	3.34	5.29	4.
P_2O_5	0.38	0.24	0.67	0.89	0.84	1.06	0.62	0.09	0.32	0.31	0.03	0.50	0.
$H_2O(+)$	0.33	0.56	0.20	0.48	1.10	0.59	tr	0.14	tr	0.11	0.42	0.48	0.
$H_2O(-)$	0.41	0.75	0.37	0.67	0.15	0.83	0.39	0.18	0.15	0.17	0.22	0.47	0.
CO_2	0.16	0.28	0.22	0.20	0.02	0.46	0.19	0.06	0.15	0.34	0.26	tr	0.
Total	100.65	100.55	99.76	99.70	100.06	100.20	100.27	100.12	100.24	99.80	100.09	100.56	99.

$Mg/Mg+Fe''+Fe'''+Mn\times100$

	50.8	51.6	59.2	61.3	45.9	60.5	64.9	40.0	0.0	29.3	15.4	37.2	36

C. I. P. W. (molecular) Norm

q	7.5	—	—	—	5.3	—	0.8	26.9	20.4	21.1	37.8	9.8	26
or	18.0	10.5	43.5	35.5	39.0	36.5	42.5	30.0	36.0	26.5	20.0	32.0	29
ab	46.5	51.5	33.5	26.5	32.0	23.0	28.5	32.5	34.0	38.5	34.5	35.5	32
an	10.3	17.5	4.0	4.8	4.5	2.3	3.8	6.5	8.3	5.0	6.3	7.3	6
ol	—	4.8	2.1	6.0	—	9.6	—	—	—	—	—	—
hy	7.2	3.2	3.0	7.0	10.4	5.2	3.4	2.0	—	1.0	—	4.8	2
di	3.2	10.0	10.0	14.4	5.2	19.2	17.6	0.8	—	3.2	—	4.4	1
mt	1.2	1.4	1.7	2.3	2.2	1.8	1.1	0.6	0.2	2.3	1.1	3.3	1
il	1.0	0.8	1.0	1.6	2.2	1.2	1.0	0.4	—	1.0	0.2	2.0	0
ap	0.8	0.5	1.3	1.9	1.9	2.1	1.3	0.3	0.5	0.5	—	1.1	0
ne	—	—	—	—	—	—	—	—	—	—	—	—

YA303 : Pyroxene-biotite gneiss from massif A.
YA285 : Enderbitic gneiss from massif A.
YE 54 : Pyroxene syenite from massif E.
YC238 : Porphyritic pyroxene syenite from massif C.
YA292 : Pyroxene syenite from massif A.
YA301 : Ditto.
YF 87 : Ditto from massif F.
YD320 : Migmatitic gneiss from massif D.
YD335 : Biotite granite from massif D.
YC310 : Granitic gneiss (nebulitic gneiss) from massif C.

YD224 : Granitic gneiss (nebulitic gneiss) from m
YB261 : Granitic gneiss (augen gneiss) from mas
YB278 : Granitic gneiss (augen gneiss) from mas
YB265 : Microcline granite from massif B.
YC313 : Microcline granite from massif C.
YD333 : Microcline granite dike from massif D.
YG 59 : Basic granulite layer from massif G.
YC307 : Pyroxene amphibolite layer from massif
YB253 : Biotite amphibolite dike from massif B.
YC318 : Pyroxene amphibolite dike from massif

Analyst : Yo

* Chiefly chlorite, sericite and calcite.

11.3	—	—	—	—	—	—	—	—	—	23.9	—	—	10.1
0.4	—	—	—	—	—	—	—	—	—	10.1	—	—	—
0.8	0.2	0.3	0.3	tr	0.5	0.1	0.5	tr	tr	tr	1.4	0.3	0.8
tr	tr	tr	0.1	tr	0.2	tr	0.4	tr	tr	tr	0.3	0.1	tr
—	tr	tr	0.8	tr	0.1	0.5	tr	tr	—	—	1.6	0.2	0.8
0.7	0.2	0.9	1.5	tr	0.9	0.1	0.5	0.5	tr	tr	0.4	tr	tr
—	1.1	0.1	1.1	0.7	1.3	—	0.4	1.2	0.7	0.6	0.3	1.8	—
100.0	100.0	99.9	99.9	100.2	100.1	100.0	100.5	97.7	100.0	100.0	100.0	99.9	99.7

60.15	73.13	71.25	69.29	77.24	61.69	71.51	72.06	71.63	70.80	50.82	59.19	52.02	50.18
0.69	0.24	tr	0.64	0.14	1.39	0.54	0.44	0.24	0.64	0.89	1.43	1.54	1.30
14.54	13.78	15.84	13.53	11.96	14.86	13.32	13.97	13.76	13.04	10.96	13.57	13.79	7.19
1.03	0.55	0.16	2.06	0.92	3.23	1.23	1.12	1.39	1.10	1.45	3.62	2.32	6.91
2.44	1.08	0.16	1.77	0.49	3.40	1.42	0.92	0.89	3.51	9.08	3.95	5.27	6.81
0.04	tr	tr	0.02	tr	0.07	0.01	tr	tr	0.04	0.18	0.15	0.12	0.18
3.63	0.55	tr	0.83	0.11	2.03	0.74	0.41	0.05	0.64	13.34	2.51	5.25	9.21
6.10	1.75	2.31	2.09	1.12	3.25	1.93	1.13	1.36	1.52	8.07	4.44	6.91	7.48
3.23	3.58	3.77	4.25	3.75	3.90	3.49	3.60	3.75	3.49	2.14	3.06	2.64	1.89
7.22	4.99	6.13	4.39	3.34	5.29	4.92	5.36	5.51	4.20	2.27	6.20	6.31	6.50
0.62	0.09	0.32	0.31	0.03	0.50	0.16	0.12	0.09	0.14	0.05	0.92	1.10	1.36
tr	0.14	tr	0.11	0.42	0.48	0.08	tr	0.04	0.31	0.27	0.32	0.53	0.85
0.39	0.18	0.15	0.17	0.22	0.47	0.42	0.66	0.38	0.27	0.38	0.25	0.94	0.24
0.19	0.06	0.15	0.34	0.26	tr	0.13	0.03	0.37	0.18	0.11	tr	0.68	0.03
00.27	100.12	100.24	99.80	100.09	100.56	99.90	99.82	99.46	99.88	100.01	99.61	99.42	100.13

64.9	40.0	0.0	29.3	15.4	37.2	36.7	28.6	5.6	19.6	69.4	55.6	37.9	55.5

0.8	26.9	20.4	21.1	37.8	9.8	26.1	26.5	25.1	27.2	—	8.2	—	—
42.5	30.0	36.0	26.5	20.0	32.0	29.5	32.0	33.0	25.5	13.0	37.5	38.5	39.0
28.5	32.5	34.0	38.5	34.5	35.5	32.0	33.0	34.5	32.0	19.0	28.0	24.5	—
3.8	6.5	8.3	5.0	6.3	7.3	6.8	4.5	4.5	6.5	13.5	5.0	7.0	(ac)13.2
—	—	—	—	—	—	—	—	—	—	21.0	—	8.4	16.2
3.4	2.0	—	1.0	—	4.8	2.2	—	(wo)0.4	—	10.8	3.8	0.2	0.8
17.6	0.8	—	3.2	—	4.4	1.2	—	0.4	—	20.0	9.2	16.4	23.2
1.1	0.6	0.2	2.3	1.1	3.3	1.2	1.2	1.5	1.2	1.5	4.1	2.6	2.4
1.0	0.4	—	1.0	0.2	2.0	0.8	0.6	0.4	1.0	1.2	2.4	2.2	1.8
1.3	0.3	0.5	0.5	—	1.1	0.3	0.3	0.4	0.3	0.3	1.9	2.4	2.9
—	—	—	—	—	—	—	—	0.3	—	—	—	—	0.6

YD224 : Granitic gneiss (nebulitic gneiss) from massif D.
YB261 : Granitic gneiss (augen gneiss) from massif B.
YB278 : Granitic gneiss (augen gneiss) from massif B.
YB265 : Microcline granite from massif B.
YC313 : Microcline granite from massif C.
YD333 : Microcline granite dike from massif D.
YG 59 : Basic granulite layer from massif G.
YC307 : Pyroxene amphibolite layer from massif C.
YB253 : Biotite amphibolite dike from massif B.
YC318 : Pyroxene amphibolite dike from massif C.

Analyst : Yozo CHIBA

IV. GRANITIZATION AND METABASITES

Various modes of occurrence of migmatization and granitization are recognized everywhere in massifs B, C, D and E, in the central part of the mountains. The succession of the granitization is represented by the series banded gneiss→augen gneiss, nebulitic gneiss→microcline granite. In massif E there is another type of granitization, the transition from pyroxene syenite to pyroxene-bearing granite towards east without any dynamic effects. On the other hand, the granitic gneiss of massif D, especially of its northeastern portion, contains uralitic hornblende as well as clinopyroxene. It seems likely that the gneiss may have been converted from the porphyritic pyroxene syenite, since the northern extension of the granitic gneiss is occupied by the porphyritic pyroxene syenite of massif E. In massifs C and B in the southern extension, the granitic gneiss exhibits mineral paragenesis of an amphibolite facies. The metamorphic grade of the granite gneiss thus increases towards the north from massif B.

The change in mineral composition of the granitic gneiss parallels that of the metabasite layers intercalated in the gneisses.

Mineral assemblages of metabasite interlayers.

a) Basic granulite:

Biotite-orthopyroxene-clinopyroxene-potassium feldspar in pyroxene syenite of massif E.

Biotite-orthopyroxene-clinopyroxene-plagioclase in biotite granite of massif D.

b) Pyroxene amphibolite:

Hornblende-orthopyroxene-clinopyroxene-potassium feldspar-quartz in granitic gneiss of massif D.

Biotite-hornblende-orthopyroxene-clinopyroxene plagioclase in pyroxene syenite of massif C.

c) Biotite amphibolite:

Biotite-hornblende-potassium feldspar-quartz in granitic gneiss of massif C.

Biotite-hornblende-potassium feldspar-plagioclase-quartz in granitic gneiss of massif B.

Biotite amphibolites usually contain sphene. Their mineral composition also belongs to the amphibolite facies, like that of the host granitic gneiss of massifs C and B. In the northern portion of massif D, clinopyroxene and orthopyroxene appear and sphene disappears in the metabasite layers, here com-

posed of pyroxene amphibolite in the granitic gneiss. This signifies that the metamorphic grade of the metabasite interlayers increases towards the north within roughly the same horizon, and represents the transition to a granulite facies. The structural and petrographical investigations have revealed that the change in the metamorphic grade does not suggest a progressive metamorphism from an amphibolite facies to a granulite facies, but a somewhat retrogressive granitization to granitic gneiss.

The metabasite layers included as xenolithic fragments in a 70 cm wide, microcline granite dike in massif D, exhibit the biotite amphibolite paragenesis and contain sphene, in spite of the pyroxene amphibolite association in the metabasite layers within the enclosing gneiss. This may indicate that the pyroxene amphibolite was converted into the biotite amphibolite under the temperature conditions of the microcline granite emplacement; i. e., under the amphibolite facies conditions.

Biotite is one of the major constituents of the metabasite layers and has variable pleochroism. Its refractive indices are generally higher in the biotite amphibolite than in the basic granulite, which, as shown in Fig. 16, agree with the indices of the hornblende.

Hornblende appears in the pyroxene amphibolite and the biotite amphibolite, and its pleochroism changes from brownish green to bluish green with decreasing metamorphic grade. A $2V_x$-N_z diagram of hornblende in the metabasites and other rocks is plotted in Fig. 17. There is a general tendency for the axial angle to decrease and for N_z to increase with decreasing metamorphic grade of the rock. At the same time, the SiO_2 content of the host rock tends to increase. These changes in refractive indices are the same as those of the biotite (Fig. 16).

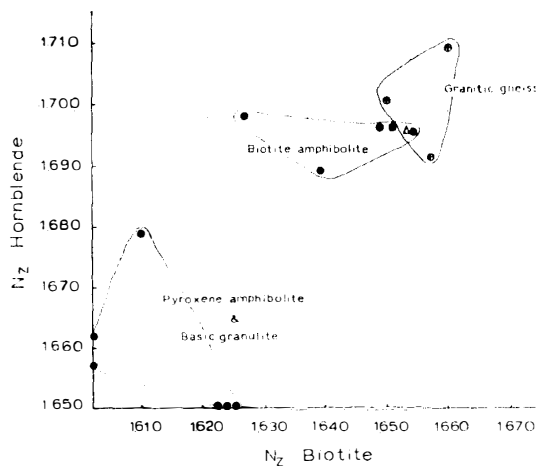The clinopyroxene in the pyroxene amphibolite shows somewhat stronger

Fig. 16. Relation between the refractive indices (N_z) of biotite and coexistent hornblende. Solid circles on the base line represent hornblende or biotite not associated with biotite nor hornblende.
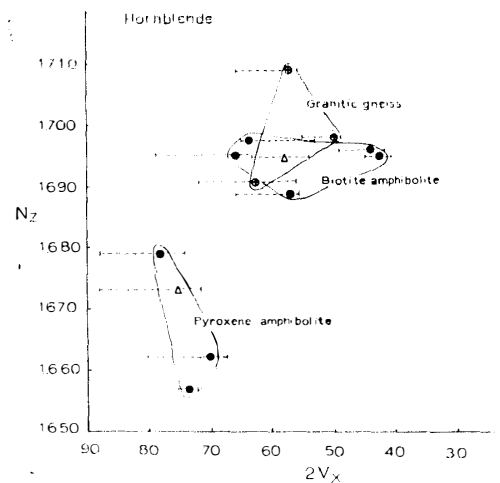
Fig. 17. $2V_x$-N_z diagram of hornblende.

pleochroism than that in the basic granulite. The $2V_z$-N_z diagram shows that the optical properties of the clinopyroxenes in the basic granulites, which are in a lower compositional field than are those in the other charnockitic rocks, indicate diopsidic composition (Fig. 18). The pyroxene amphibolite contains salitic pyroxene which is higher in Fe/Mg than that in the basic granulite, as one expects from the lower metamorphic grade. The orthopyroxene which has lower refractive indices than that of the enclosing pyroxene syenite is optically determined to be hypersthene.

Variation of the An content of plagioclase is very small and the An content is rather constant, being 23% when potassium-feldspar coexists, even in the basic granulite. The pyroxene amphibolite without potassium-feldspar contains plagioclases of An 30 and An 43 as average compositions, with a maximum of An 51.

Basic dikes are metamorphosed to metabasite of various types.
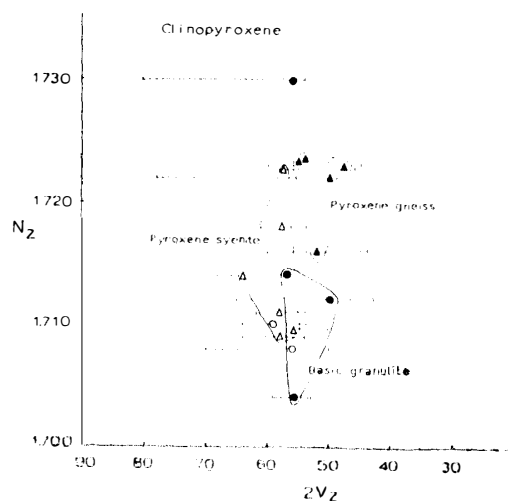
Fig. 18. $2V_z$-N_z *diagram of clinopyroxene.*

The mineral assemblages of the dikes are as follows:

Biotite-clinopyroxene-plagioclase-potassium feldspar-quartz in pyroxene syenite in massif C.

Biotite-hornblende-clinopyroxene-plagioclase-potassium feldspar-quartz in granitic gneiss in massif C.

Biotite-hornblende-plagioclase-potassium feldspar-quartz in granitic gneiss in massif B.

Since all of the metabasites carry sphene, these assemblages are placed in the amphibolite facies of massif B, and in the upper amphibolite facies of massif C. The gneissosity of these rocks is so intense that they may be called pyroxene-biotite gneiss and hornblende-biotite gneiss or schist. The optical characteristics of the clinopyroxene ($2V_z = 56°$, $N_z = 1.708$; $2V_z = 59°$, $N_z = 1.710$) are such that expected in the basic granulite field, according to the $2V$-N_z diagram (Fig. 18), whereas the refractive indices of the biotite ($N_z = 1.664$, 1.652) are rather similar to those of the biotite in the granite gneiss. The An content of the plagioclase

is invariably An 23± as in the metabasite interlayers because of the co-existence of potassiumfeldspar (KIZAKI, 1964).   It is clear, therefore, that in massif C these dikes were metamorphosed under the upper amphibolite facies conditions when the microcline granite and pegmatite were intruded subsequent to their emplacement.   The metamorphic grade of the metabasite layers tends to increase towards the north from massif B.   Although the origin of the metabasite layers in the gneiss complex remains conjectural, the clean-cut form of metabasite dikes having a width up to several meters is sufficient to negate the possibility of their deriving from sedimentary rocks.   They may have originated as basaltic or doleritic dikes, but their chemical compositions are conspicuously different from the average chemical compositions of basaltic rocks (ENGEL and ENGEL 1962, p. 63).   The most notable differences are low contents of CaO and FeO and especially high content of K_2O in the metabasite dikes as well as in the metabasite interlayers of this complex.   It seems likely that a potassium metasomatism took place in the metabasite interlayers and meta-dikes, resulting in general enrichment of biotite and potassium-feldspar.

PICHAMUTHU summarized the characteristics of charnockitic dikes similar to this type as follows, " The charnockitic dykes are metamorphosed representatives of the earliest formed basic dykes.   They are granulitic without chilled selvages and non-transgressive " (PICHAMUTHU, 1953, p. 147).   He stated that the agency which caused this metamorphic effect is considered to be the palingenetically formed, later charnockites.   The agency in question, however, may have been post-kinematic microcline granite accompanied by microcline pegmatite and their potash metasomatism under the amphibolite facies conditions.

V. CHARNOCKITIC GROUP

The charnockitic group is composed of pyroxene-biotite gneiss, enderbitic gneiss, charnockitic gneiss, porphyritic pyroxene syenite and pyroxene syenite except metabasites.

The interrelation between the charnockitic gneisses of massif G and the porphyritic pyroxene syenites of massifs E and F has not been determined, because of lack of outcrops. The charnockitic gneisses of massif G have a banded structure, rather similar to a lit-par-lit injection gneiss, with the alternating basic and acidic layers. In detail, however, the transition from basic to acidic layers is represented by a gradual increase in the amount of potassium-feldspar and quartz, accompanied by grain growth and an increase in Fe/Mg or Ti in biotite (suggested by the changes in the refractive indices of biotite, clinopyroxene and orthopyroxene). It is in harmony with the increase of acidity in the host rocks in general (Table 4). It is, therefore, conceivable that the acid charnockite may have been produced metasomatically from the intermediate or basic charnockite.

The field relations between the porphyritic pyroxene syenite of massif C and the pyroxene syenite of massif A have not been determined either. The latter looks like an igneous intrusive in the field and under the microscope. In massif A, a large quantity of angular fragments of pyroxene-biotite gneiss and enderbitic gneiss are included in the pyroxene syenite, and the foliation and arrangement of these fragments is parallel to that in the pyroxene gneiss in the southern part of the massif. This fact suggests a structurally harmonic emplacement. The mineral assemblages of these rocks are rather similar to each other, as follows:

Pyroxene-biotite gneiss:

Biotite-potassium feldspar-clinopyroxene-orthopyroxene plagioclase-quartz-(hornblende)

Enderbitic gneiss:

Plagioclase-biotite-clinopyroxene-orthopyroxene-potassium feldspar-quartz

Pyroxene syenite:

Potassium feldspar-biotite-hornblende-clinopyroxene-orthopyroxene-plagioclase-quartz

Modal relations between the gneisses and the syenite show an increase in potassium-feldspar, biotite and hornblende, with the simultaneous decrease of quartz, plagioclase and pyroxene from the former to the latter. The pyroxene

syenite is characterized by the presence of hornblende, subhedral potassium-feldspar with Carlsbad twinning, and unstable pyroxenes which have been partially altered to biotite in some places.

It is clear that the pyroxene syenite contains more K_2O (Figs. 13 and 14) and MgO (Fig. 15, Table 12) than do the pyroxene gneisses.

Table 12. $100 \times Mg/(Mg + Fe'' + Fe''' + Mn)$ in the charnockitic rocks.

Pyroxene biotite gneiss	Enderbitic gneiss	Pyroxene syenite		Porphyritic pyroxene syenite		
YA 303	YA 285	YA 292	YA 301	YE 54	YC 238	YE 87
50. 8	51. 6	45. 9	60. 5	59. 2	61. 3	64. 9

One of the pyroxene syenites of massif A (YA292) has less $Mg/(Mg + F'' + F''' + Mn)$ them any of the gnisses, because it contains hardly any pyroxene, but contains abundant hornblende instead. The optical properties of the hornblende and biotite place them in the compositional field of those in granitic gneiss (Figs. 16 and 17). This seems to indicate amphibolite facies conditions. However, the other sample (YA301) from the same massif has a high MgO content (Table 12), because of a smaller amount of hornblende and an abundance of pyroxene. Though orthopyroxene is not so abundant, it is an important index mineral of the granulite facies. The pyroxene gneisses can be clearly separated from the pyroxene syenite by means of the $2V-N_z$ diagram of orthopyroxene (Fig. 19).
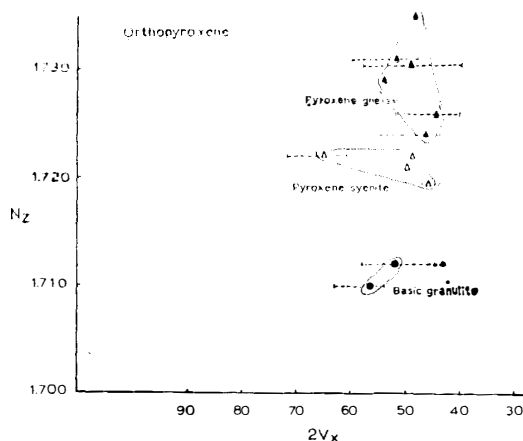

Fig. 19. $2V_x-N_z$ diagram of orthopyroxene.

The orthopyroxene in the pyroxene gneiss is optically shown to be ferrohypersthene, and that in the pyroxene syenite to be hypersthene.

Clinopyroxene is more abundant than orthopyroxene. The compositional field of the pyroxene gneisses is separated from that of the pyroxene syenite, as seen in the $2V-N_z$ diagram (Fig. 18). The refractive indices of the clinopyroxene in the pyroxene syenites, however, are similar to those of the clinopyroxene in the pyroxene gneisses of massif A but the discrimination can be made by their

axial angles. The pyroxene in the pyroxene gneiss is salitic and augitic whereas that in the pyroxene syenite is salitic and diopsidic, as judged from optical properties.

The biotite is invariably reddish brown, and its refractive indices in the pyroxene gneisses ($N_z = 1.667$, 1.671) are higher than in the pyroxene syenite ($N_z = 1.666$, 1.653). Plagioclase has a rather narrow compositional range between An 21 and An 28, the average value through the gneisses and syenites being An 24.

Optical measurements of the mafic minerals show a decrease in Fe/Mg from the gneiss to the syenite, with a little change in the SiO_2 content, except for sample YA292. The mineral paragenesis of these rocks imply granulite facies conditions, and the similarity of petrography and structure between the pyroxene gneisses and the pyroxene syenite suggests a close genetic relationship between the two. The ACF diagram shows the different paragenesis of the pyroxene gneisses and hornblende-bearing pyroxene syenite of the granulite facies in massif A (Fig. 20).
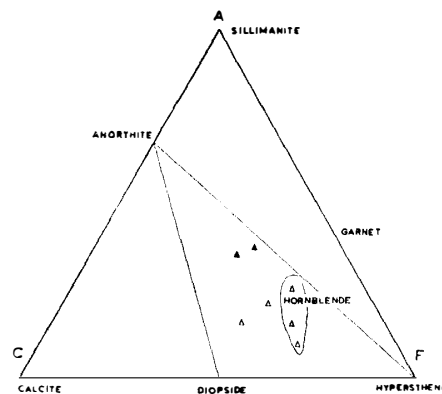

Fig. 20. ACF diagram of the charnockitic group.

It seems likely that the intrusive pyroxene syenite of massif A is the product of palingenesis of the pyroxene gneisses. CROHN (1959) and KLIMOV et al (1963) suggest the presence in the McRobertson Land and the Mirny region of East Antarctica of intrusive charnockite resulting from palingenesis and rheomorphism.

VI. SUMMARY

The rocks in this mountain region may be divided into two groups: a charnockitic group and a granitic group, on the basis of their petrography, petrochemistry, and structure. The charnockitic group is involved in the older complex which crystallized under the granulite facies conditions. It has been partly modified by later granitization, attributed to the granitic group which occupies the central part of the region and shows various grades of granitization. The grade of metamorphism increases towards the north, parallel to the gneissosity. The intercalated metabasite layers have the same mineral paragenesis as the host rocks.

Basic dikes intruded obliquely to the granitic gneisses and the pyroxene syenites were metamorphosed into a variety of metabasites under amphibolite facies conditions, probably related to the subsequent intrusion of microcline granite and microcline pegmatite. They show strong gneissosity parallel to the boundary. This metamorphism may be a potash metasomatism accompanied by some stress. It is not a regional dynamometamorphism.

A thrust movement represents the last stage of the structural evolution. The thrust plane is roughly parallel to the foliation of the migmatitic and granitic gneisses. Hence, the thrust fault may have originated from the differential movement associated with the formation of these gneisses.

References

CROHN, P. W. (1959): A contribution to the geology and glaciology of the western part of Australian Antarctic Territory. ANARE Reports, Ser. A, Vol. III, 102.

ENGEL, A. E. J. and ENGEL. C. G. (1962): Progressive metamorphism of amphibolite, northwest Adirondack Mountains, New York. Geol. Soc. Amer. Buddington vol. 37–82.

ESKOLA, P. (1963): The Precambrian of Finland. The Precambrian, Vol. 1, edited by K. Rankama. Intersci. Pub.

FUJIWARA, K. (1964): Preliminary report on the morphology of the inland ice sheet of the Mizuho Plateau, East Antarctica. Antarctic Record, No. 23, 1–11.

KIZAKI, K. (1964): Tectonics and petrography of the East Ongul Island, Lützow-Holm Bukt, Antarctica. JARE Sci. Rep., Ser. C, No. 2, 1–24.

KLIMOV, L. V., RAVICH, M. G. and SOLOVIEV, D. S. (1963): East Antarctic charnockites. SCAR-IUGS symposium on Antarctic geology. Cape Town.

PICCIOTO, E. and COPPEZ, A. (1964): Bibliographie des mesures d'ages absolus en Antarctique. (Addendum août 1963). Ann. Soc. Geol. Belgique, 87, 115–128.

PICHAMUTHU, C. S. (1953): The charnockite problem. Mysore Geol. Asosc. India.

SHIBUYA, G. and KIZAKI, K. (1965): On some minerals collected by JARE 1960–1961, in press.

TATSUMI, T., KIKUCHI, T. and KIZAKI, K. (1963): Geology of the region around Lützow-Holm Bay and Yamato Mountains, Antarctica. SCAR-IUGS Symposium on Antarctic geology, Cape Town.

TUTTLE, O. F. and BOWEN, N. L. (1958): Origin of granite in the light of experimental studies in the system $NaAl_3O_8$-$KAlSi_3O_8$-SiO_2-H_2O. Geol. Soc. Amer. Mem. 74.

TILLEY, C. E. (1936): Enderbite, a new member of the charnockite series. Geol. Mag. 73, 312–316.

WEGMANN, E. and SCHAER, J. P. (1962): Chronologie et deformations des filons basiques dans les formations Precambriennes du sud de la Norvege. Norsk Geol. Tidsskr. 42, 371–387.

YOSHIDA, Y. and FUJIWARA, K. (1963): Geomorphology of the Yamato (Queen Fabiola) Mountains. Antarctic Record, No. 18, 1–26, (in Japanese with English abstract).